EQUATION OF STATE MODEL DEVELOPMENT AND COMPOSITIONAL SIMULATION OF ENHANCED OIL RECOVERY USING GAS INJECTION FOR THE WEST SAK HEAVY OIL

By

Ganesh G Morye

RECOMMENDED:

Dr. Santanu Khataniar

Dr. Abhijit Dandekar

Dr. Shirish Patil, Advisory Committee Chair

Chair, Dept of Petroleum Engineering

APPROVED:

Dean of College of Engineering & Mines

Dean of Graduate School

Oct 17, 2007

Date

EQUATION OF STATE MODEL DEVELOPMENT AND COMPOSITIONAL SIMULATION OF ENHANCED OIL RECOVERY USING GAS INJECTION FOR THE WEST SAK HEAVY OIL

A

Thesis

Presented to the Faculty

of the University of Alaska Fairbanks

in Partial Fulfillment of the Requirements

for the Degree of

MASTER OF SCIENCE

By

Ganesh G Morye, B. Chem. Eng

Fairbanks, Alaska

December 2007

Abstract

West Sak oil field, with its very huge reserves of heavy oil, has the potential of supplementing the declining light oil production on the Alaska North Slope. Due to the heavy nature of oil, its phase behavior is very complex. A proper understanding of the phase behavioral changes of the West Sak oil is crucial to design any enhanced oil recovery scheme. Such Enhanced Oil Recovery (EOR) techniques are essential in the absence of natural drive mechanisms in these reservoirs. For the proper selection of any EOR technique, reservoir simulation studies should prove its viability.

Accordingly, a complete phase behavior analysis of the West Sak crude oil was carried out. All the available experimental data was scrutinized and a model equation of state was developed that should describe the phase behavior of West Sak oil. After having done that, reservoir simulation was carried out to study the implications of employing gas injection as an EOR technique for the West Sak reservoir. It was found that a definite increase in heavy oil production can be obtained with proper selection of injectant gas and optimized reservoir operating parameters. A comparative analysis is provided which should help in making such a decision.

Table of Contents

Page

Page

Page

List of Figures

Page

Page

Page

List of Tables

Page

List of Appendices

Page

Acknowledgements

First, I would like to extend my sincere gratitude to my advisor Dr. Shirish Patil for his continued support in all possible ways and for being a source of inspiration. I would also like to thank my committee members Dr. Santanu Khataniar and Dr. Abhijit Dandekar for showing a keen interest in my thesis and guiding me during the entire course of this work. My sincere appreciation also goes to all the faculty, staff and fellow graduate students of the Department of Petroleum Engineering for their support. Finally, I would like to deeply thank my family for all their support and advice and I will always remain indebted to them.

Disclaimer

Chapter 1

Introduction

1.1. Overview

Over the last century, the worldwide production of crude oil has mainly concentrated on light-oil or conventional crude oil. However, declining production of oil from the available recoverable resources makes it necessary to explore other unconventional forms of crude oil, such as heavy oil, to meet the energy demands. Statistically speaking, the reserves of conventional crude oil that remains to be produced stand at one trillion barrels, whereas reserves of heavy oil and bitumen stand at more than five trillion barrels, 80 percent of which are in Canada, Venezuela and U.S. (Patil & Dandekar, 2004)

The Alaska North Slope (ANS) has two of the largest oil fields in North America, Prudhoe Bay and the Kuparuk River Unit. The answer to the energy demands of the future will be the heavy-oil formations on the ANS. Ugnu, West Sak, and Schrader Bluff formations put together hold a total of 36 billion barrels of oil (BBO) which far exceeds the original-oil-in-place of Prudhoe and Kuparuk combined. The main reason for the high viscosity of the oil in these locations is the proximity of the formations in which they occur to the permafrost. These formations are very shallow and occur at depths of 3000-3500 feet (Anna, 2005). Heavy oil consists of molecules with more than 15 carbon atoms. Heavy oils have viscosities in the range of 100-1000 cP and densities in the range of 934-1000 Kg/m^3 (Speight, 1991). ANS heavy oils are classified as "A class": medium heavy oils. Class A type oils are of high API gravity and relatively low downhole viscosity and so are more problematic to produce than the conventional light crude oil.

The West Sak is a heavy oil accumulation within the Kuparuk River Unit on ANS. The West Sak reservoir has 20 (BBO) which is as large as Prudhoe Bay's 23 billion barrels of original-oil-in-place. These heavy oil resources on ANS have received little attention, mainly because these oils are viscous, flow sluggishly in the formations, and are difficult to transport. There are numerous other problems like emulsification, cavitation and sand production during pumping, injectivity limitations to solvent and gas floods and formation damage from asphaltene precipitation (Patil & Dandekar, 2004). Consequently, producing oil from these formations is considered to be uneconomical.

A solution to these problems will be a correct understanding of the phase behavior of heavy oils. Compositions and the phase behavior of heavy oil systems are very complex. Typically, heavy oil consists of components ranging from asphaltenes to light alkanes, nitrogen, sulphur, and oxygen, primarily due to the selective removal of lighter alkanes early in the degradation process, which makes its phase behavior extremely complex. The presence of additional solvents which are used during the secondary and tertiary recovery schemes adds to the complexity of phase behavior. Correct understanding of phase behavior thus becomes very necessary for reservoir modeling and many other production related issues. To understand phase behavior of heavy oils, proper knowledge of the various physical properties of the oil such as density, viscosity, bubble point pressure is very important. Viscosity reduces the flow rate and density is influenced by chemical composition. Density is used to give rough estimations of the nature of petroleum and petroleum products. Bubble point pressure determines the nature of the phase envelope.

Equation of State (EOS) models can be used to describe the phase behavior of reservoir fluids and calculate their volumetric properties. These EOS models when used as "it is" do not accurately simulate the phase behavior because the heavy ends have uncertainties in the molecular weight and critical properties. Therefore, to simulate the phase behavior of reservoir fluids under different conditions, "tuning" of EOS is carried out. Tuning of EOS is found to be the best method for improving the predictions of compositional simulators. Tuning of EOS is generally fluid specific, the type and number of EOS parameters altered in the tuning process differs for various approaches. This tuned EOS can further be used to accurately describe the volumetric properties and the phase behavior of reservoir fluids and ultimately be used for reservoir simulation purposes.

Reservoir simulation is conducted to predict performance of different secondary and/or tertiary recovery schemes when primary recoveries are not sufficient. The various options available for carrying out tertiary recovery schemes are gas injection, thermal recovery or chemical injection. Thermal recovery methods may endanger the permafrost on the North Slope. Chemical EOR is uneconomical due to its high costs relative to the crude oil. In reservoirs with favorable rock and fluid properties, application of gas injection processes can enhance the recovery efficiency and value of field development. Miscible floods, immiscible floods, Water-Alternating-Gas (WAG) floods, are possible methods to carry out enhanced oil recovery using the gas injection process.

Miscible displacement has the advantage in that it is possible to achieve miscibility (first contact or multi contact) and an improvement in displacement efficiency. Various hydrocarbon gases called Miscible Injectants (MI's) can be

used. The increase in oil recovery is often related to the degree of leanness (methane concentration) of the injection gas. With the aid of reservoir simulators, it is possible to investigate the feasibility of different gas injection schemes. A comparison of reservoir performance under various gas injection scenarios can aid in designing the optimal conditions for reservoir operation.

1.2. Objectives

The main focus of this research is to carefully study the phase behavior of ANS crude oil from the West Sak reservoir. Following tasks are performed in accordance with the study undertaken:

i. Develop a tuned EOS model for the West Sak oil using available experimental data from a previous study.
ii. Use the tuned EOS model to carry out compositional reservoir simulation to predict performance of the West Sak reservoir for different gas injection schemes and a variety of injection gases.

Chapter 2

Literature Review

2.1. Phase Behavior of Petroleum Reservoir Fluids

There are three basic types of calculations involved in modeling a hydrocarbon system: phase equilibria, volumetric behavior, and thermo physical properties. Cubic Equations of State (CEOS) are used to predict the phase equilibria of complex non-polar hydrocarbon systems.

An EOS can be used to simulate the behavior of fluids under varying conditions when it is impractical/expensive/time consuming to carry out experiments and get the laboratory data. There are various processes encountered in a reservoir operation, like the mass transfer of components between the injection gas and reservoir fluid and many more, which dictates changes in compositions, physical properties like density, and viscosity of the fluids. An EOS can simulate these changes without the need of data points for each step change. For a displacement-like process, which is dominated by mass transfer between phases, an EOS can very well predict the compositional path of the fluids during the change. Also, there are many field projects which have similar strong composition dependence, such as production from gas/condensate reservoirs, miscible and near-miscible gas injection, or water-alternating-gas injection for enhanced oil recovery (Wang & Pope, 2001).

2.1.1. Peng-Robinson Equation of State

The most widely used cubic equation of state among researchers and engineers is the Peng-Robinson EOS (PR EOS) due to its more accurate volumetric predictions

than the Redlich-Kwong EOS and it will be used in the study. It is a two parameter EOS and is defined as follows:

$$P = \frac{RT}{V-b} - \frac{a\alpha}{V(V+b)(V-b)} \qquad (2.1)$$

Where P is the system pressure (psia), T is the temperature (°R), R is the gas constant (10.73 psi-ft3/lb-mol°R) and V is the molar volume (ft^3/lb-mol). α is the dimensionless parameter and is defined by the following expression:

$$\alpha = [1 + m(1 - T_r^{0.5})]^2 \qquad (2.2)$$

The parameter m in the equation is in turn correlated with the acentric factor as:

$$m = 0.3746 + 1.5423\omega - 0.2699\omega^2 \qquad (2.3)$$

There are two parameters, *a* and *b,* in the cubic EOS to be determined. There are two approaches to determine their values.

The first approach is the regression technique that utilizes the experimental data sets (like vapor pressure and density) to estimate the regression coefficients (a, b) of the cubic EOS. Regression analysis follows the principle of least square to fit the data with minimum error. Even with these robust techniques, properties like critical constraints (critical pressure and critical temperature) and K-values are

never estimated accurately by fitting properties like density and vapor pressure. This is mostly attributed to the inherent limitation of cubic equation of state for predicting Pressure-Volume-Temperature (PVT) behavior.

The second popular technique is to derive these coefficients using the critical constraints, unique for that fluid composition. Critical constraints provide the best tool to determine the parameters of the cubic EOS analytically. This enhances the predictability of the cubic EOS, and helps in accurately predicting the K-value, including the near critical point value. The only limitation attached to this technique is over prediction of critical compressibility factor Z_c for all components of real fluids (Twu et al., 2007).

2.2. Tuning of Equation of State

EOS models are capable of accurately predicting the phase behavior of systems having well-defined components. Defined components have well known critical properties and an acentric factor. However, real systems like the petroleum fluids are very complex and have many different hydrocarbon and non-hydrocarbon components. Apart from the well-defined components, they have some quantity of heavier fractions which are lumped together into a plus fraction, usually C_{7+} or pseudofractions, or much heavier fractions like C_{20+}. These heavier fractions are not very well defined in terms of their critical properties and acentric factors. It is very difficult to calculate and/or obtain experimentally the values of these critical properties and acentric factors leading to large errors in predictions of EOS. Liu (1999) has quantified the prediction errors in the saturation pressure in absence of a properly tuned EOS (Table 2.1).

Table 2.1: Comparisons of saturation pressures between experimental and predicted values (Liu, 1999)

Sample	T, °F	Saturation Pressure psia				
		Lab	PR	Error,%	ZJRK	Error,%
Oil 2	176	4475	3344	25	3477	22
Oil 3	140	2130	1761	17	1818	15
	160	2377	1985	16	2014	15
	180	2612	2195	16	2200	16
	200	2807	2388	15	2377	15
Oil 4	250	2572	2259	12	2300	11
Oil 5	201	3837	3311	14	3366	12
Oil 6	234	2761	2383	14	2432	12
Oil 7	131	1709	1531	10	1631	5
Gas I	181	4076	3334	18	3461	15
Gas 2	190	4465	3680	18	3593	20
Gas 3	226	4453	4547	-2	4857	-9
Gas 4	240	3375	3138	7	3246	4
Gas 5	267	4857	4494	7	4165	14
Average Error %			14		13	

Therefore, the EOS model is "tuned" for a given reservoir fluid to improve the performance of the EOS models and get more accurate predictions. Tuning is achieved by matching the available experimental data with the EOS model predictions by changing (regressing) different parameters. The parameters that are regressed to get a fit are usually critical properties of the heavier fractions. A general verifying point for such kind of regression is the matching of saturation pressures. Saturation pressures become important in phase behavior analysis as

they define the shape of the phase envelope. A tuned EOS can lead to better predictions of the volumetric and phase behavior of reservoir fluids, which in turn leads to better predictions of compositional reservoir simulators.

2.2.1. Tuning Procedure

The following schematic for developing an EOS model representing a given fluid system was given by Wang & Pope (2001). It involves the following steps:

1. Develop pseudocomponents for the heavy fraction.
    a. Split the heavy fraction into many pseudocomponents by use of a distribution function that honors the measured Molecular Weight (MW) and Specific Gravity (SG). The MW and SG of each split pseudocomponents are obtained.
    b. Estimate the critical temperature *(Tc),* critical pressure *(Pc), and* acentric factor (ω) for these split pseudocomponent by use of an empirical correlation.
    c. Lump these split pseudocomponents into a few groups.
    d. Compute the *Tc, Pc, and* ω for these lumped groups by use of mixing rules.
2. Validate this EOS model against experimental PVT data and determine if tuning of the EOS parameters is needed.
3. Tune the EOS parameters.
    a. Select suitable experimental data to tune the EOS.
    b. Choose the adjustable EOS parameters that will be used to match this data.

c. Perform tuning by use of optimization technique or simulation software.

4. Evaluate the predictive capability of this EOS model.

2.2.1.1. Splitting the Plus Fraction

Splitting the plus fraction is invariably the first step that is performed in any EOS modeling. This is because the plus fraction can contain and indefinite number of components whose properties are represented just by the molecular weight and specific gravity. This data is obtained experimentally and can have large errors leading to erroneous predictions by the EOS. Therefore, characterization or splitting of this plus fraction into well defined components is essential. There are various procedures cited in the literature for splitting of the plus fraction. The three most widely used methods in the industry, due to their ease and simplicity are:

- Exponential
- Two-Stage Exponential
- Gamma Distribution

Exponential Distribution Function (Katz, 1983)

This method requires only the mole fraction of C_{7+} and is given by:

$$z_n = 1.38205 \, . \, z_{c_{7+}} \, . \, e^{-0.25903n} \qquad (2.4)$$

This function holds most appropriately for gas condensates and lighter fluids.

Two-Stage Exponential (Katz, 1983)

In this method the gamma function is approximated to make it suitable for black-oil fluids.

Gamma Distribution (Whitson, 1983)

This is a three parameter gamma probability distribution function and is suitable for all fluid types. In this method, the probability distribution method is used to relate the mole fraction and molecular weight of SCN components of the plus fraction and is given by:

$$p(x) = \frac{exp[-(x-n)/\beta](x-n)^{\alpha-1}}{\beta^{\alpha}.\gamma(\alpha)} \qquad (2.5)$$

Where α, n, β are parameters defining the distribution and determined from the available analytical information. γ is the gamma function.

2.2.1.2. Critical Properties Correlation

CMG Winprop is an EOS modeling software and is discussed in detail in Section 2.3. It provides the option of three correlations for calculating the critical properties:

1. Lee-Kesler (Kesler & Lee, 1976)
2. Riazi (Riazi & Daubert, 1980)
3. Twu (Twu , 1984)

The Twu correlation is based on a corresponding state principle and is found to be most appropriate for heavy oil fractions.

2.2.1.3. Grouping Schemes

The basic input data to any reservoir simulator is the complete composition analysis and its phase behavior as modeled by the EOS. A major limiting factor for such kind of simulation software is the simulation time or the computing time. Simulation time increases exponentially with the increase in the number of components. It is possible to describe a given fluid with fewer numbers of components without significantly compromising the predictive ability of the reservoir simulator. Reduction in the number of components can be achieved by a process called lumping in which several components are represented by a single component, the pseudocomponent. Lumping might lead to inconsistent results if it is not carried out properly. Therefore, lumping becomes crucial if EOS has to make accurate predictions. The lumping into pseudocomponents usually consists of two steps: (Joergensen & Stenby, 1995)

1. Selection of pseudocomponent groups
2. Calculation of physical properties of these components.

There are a number of lumping schemes. The more simplistic and traditional are based on *equality of mole fractions* and *equality of weight fractions* (Joergensen & Stenby, 1995). Whitson (1983) proposed a technique for estimating the number of Multi-Carbon-Number (MCN) groups needed for adequate plus-fraction description, as well as which Single-Carbon-Number SCN) groups belong to the MCN group. The number of MCN groups, *Ng* is given by:

$$N_g = Int[1 + 3.3log_{10}(N - n)] \qquad (2.6)$$

The molecular weights separating each MCN group are taken as and are given by:

$$M_I = M_n\{exp[(1/N_g)ln(M_N/M_n)]\}^I \qquad (2.7)$$

Where M_N is the molecular weight of the last SCN group and I =1, 2..... N. Molecular weights of the SCN groups falling within the boundaries of these values are included in the MCN group, *I*.

2.2.1.4. Tuning Parameter Selection

Tuning an EOS can be very expensive in terms of man-hours involved. Since tuning is an "art", the way an EOS can be tuned will vary from individual to individual. Thus the outcome of such a tuning process can be entirely different for two individuals. The vast pool of parameters that can act as "tuning parameters", augmented by the equally vast pool of experimental data points, adds to the complexity of a tuning process. For a simplistic approach, the parameters that can be tuned are *omega a* and *omega b*, critical temperature T_C, acentric factor A_c, volume correction parameter V_{cn}, molecular weight *MW*, and binary interaction coefficients *(BIN)*. Thus, for a 10-component system, we have an assembly of as many as 105 data points. The test lab data to be matched may include those from separator test (SEP), constant composition expansion (CCE), differential liberation (DIF), swelling test (SWT), saturation pressure test (SAT), and a variety of miscibility tests. Each laboratory test may run at different times at different experimental temperatures for different fluid samples. Therefore, there may be as few as one experimental data point or as many as hundreds of data points (Liu, 1999). Hence,

the tuning of all these parameters by use of a regression program may break the internal consistency among them and result in a substantial loss of predictive power of the EOS. A reasonable guideline is to tune as few parameters as possible and to tune them as little as possible to achieve an acceptable match with the data while still maintaining internal consistency among the parameters (Wang & Pope, 2001).

Coats & Smart (1986) have made some important observations involving manual EOS-tuning processes:

- ∇ Do not include any regression variable that, by inspection, can have only a negligible effect on calculated results.
- ∇ Use an optimal regression variable set. Too many variables may result in nonconvergence of nonlinear regression or a drift of regression to the maximum number of iterations. Too few regression variables may yield poor match to the laboratory data.
- ∇ The characteristics of an optimal regression variable set are that the regression converges; the variable values converged upon are realistic; deletion of any member of variable set results in either or both of (1) a significant worse match and (2) unrealistic variable values; and addition of any other EOS parameters results in either or both of (1) nonconvergence and (2) insignificantly better data match.

Al-Meshari et al., (2005) provides a step by step guideline that can be adopted for tuning an EOS:

1. Split the laboratory plus fraction to SCN groups, usually up to SCN 44; the

last component will be C_{45+}.

2. Use correlations which are usually functions of normal boiling point temperature and specific gravity, to estimate the critical properties and acentric factor for each SCN group.
3. Match the saturation pressure at reservoir temperature using the extended composition.
4. Group SCN groups to MCN groups.
5. Assign critical properties and acentric factor for each MCN group.
6. Match the saturation pressure at reservoir temperature using the grouped composition.
7. Match the volumetric data by regression of the EOS parameters.

2.3. WinProp

WinProp is CMG's equation of state multiphase equilibrium property package featuring fluid characterization, lumping of components, matching of laboratory data through regression, simulation of multiple contact processes, phase diagram construction, solids precipitation, and more. Laboratory experiments considered in WinProp include recombination of separator oil and gas, compressibility measurements, constant composition expansion, differential liberation, separator test, constant volume depletion and swelling test.

WinProp can be used to analyze the phase behavior of reservoir gas and oil systems, and to generate component properties for CMG's compositional simulator Generalized Equation of state Model (GEM), Implicit-Explicit black oil simulator (IMEX) and steam and additives thermal simulator STARS.

WinProp contains a graphical interface that allows the user to prepare data, run the phase property calculation engine, view the output with an editor, and create plots with Microsoft Excel™.

2.4. West Sak Reservoir

The West Sak reservoir overlies the Kuparuk formation in the Kuparuk River Unit and is spread over an area of 260 sq miles (DeRuiter et al., 1994). Sharma (1993) has given a comprehensive description of the West Sak reservoir.

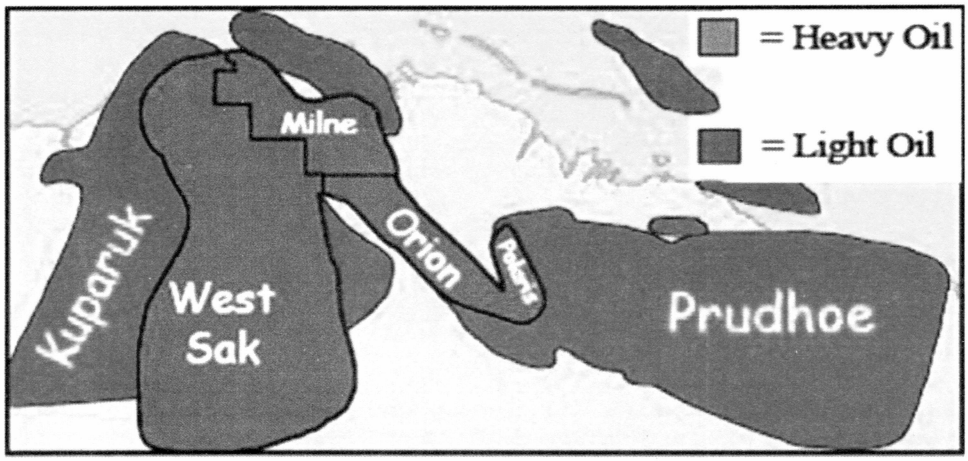

Figure 2.1: West Sak location (reconstructed from Targac et al.,2005)

The main challenge that the operators in West Sak reservoir face has been the economical production of these extremely viscous oils. Although waterflooding has been quite successful for the production of these heavy oils, the petroleum industry is on the lookout for alternative means of development like miscible or immiscible gas injection. The viability of any new technique should first be proven on a laboratory scale before its field applications. Such a study will require extensive geological and petrophysical data to simulate the actual reservoir

conditions. Reservoir property values like water saturation, porosity, and permeability comprise such a data set.

2.4.1. Geologic overview (Sharma, 1993)

Deposited during the late cretaceous and early tertiary, the West Sak sands are shallow marine and deltaic complex sands. Due to their great lateral continuity, they are of great economic importance. The Kuparuk River Unit and Milne Point Unit are both situated between the depths of 2,000 and 4,500 ft (1,141 m to 1,231 m) below sea level, and are the main oil bearing horizons within these sands.

The West Sak Sands can be broadly divided into two members, the upper and lower. The average thickness is about 300 ft (91 m) in the Kuparuk River Unit and Milne Point Unit areas. The lower member exhibits individual sands beds with thicknesses ranging from 0.2 ft to 5 ft. The individual units characteristically show the presence of ripple bedding and hummocky cross stratifications. These are in turn inter-bedded with siltstone and mudstones. Bioturbation is also seen. The upper member exhibits two distinctly divided and continuous sand units, each about 25 ft to 40 ft thick. The main sedimentary structures seen in this member include massive beds with planar bedding and low-angle cross bedding.

With the help of logs and core samples, a basic cross section of the sands can be visualized. The upper sands are divided into two members, while the lower sands are divided into four members. Thus the 6 individual sands occur as follows:

1. Upper West Sak Sand Member
    - Sand 1
    - Sand 2

2. Lower West Sak Sand Member
    - Sand 1
    - Sand 2
    - Sand 3
    - Sand 4

2.4.2. Petrophysical Properties (Sharma, 1993)

Porosity values of the West Sak Sands vary a lot, ranging from as low as 15% to as high as 40%. The water saturation of the sands ranges from about 9% to as high as 46%. Net pay thickness ranges from 1 ft to about 37 ft.

From the petrophysical data and its subsequent analysis, it can be seen that the two individual sands of the Upper West Sak sand member are the best reservoirs. Their porosity values are high and similar to the first two members (Sand 1 and Sand 2) of the Lower Member. But, the percentage water saturation in the Lower Member sands is noticeably higher. In Lower Sand 3, the water saturation is sometimes seen to be as high as 80%. The Lower Sand 4 is discontinuous. Also the net pay thickness is less in the Lower Sands, in many cases less than 10 ft.

This difference in the petrophysical characteristics of the Upper and Lower Sand members has been attributed to their different depositional histories. The upper sands were deposited in shallow marine and delta front environments, resulting in cleaner and thicker sands, as compared to the Lower Sands which were deposited in the shelf depositional environment.

2.5. Enhanced Oil Recovery (Green & Willhite, 1998)

Oil recovery operation primarily utilizes the natural pressure energy of the reservoir in order to produce oil. Low recovery and small life span are problems with such reservoirs. To enhance the productivity and life span of the reservoir, the industry started practicing secondary and tertiary/enhanced oil recovery methods.

The secondary oil recovery method, the second stage of operation usually follows the primary production decline. Waterflooding has been identified as the best example of a secondary recovery process. There have also been instances where waterflooding has been used as the primary oil recovery method. Another example of a secondary recovery method is gas injection. Waterflooding utilizes the lower mobility in order to increase the overall recovery efficiency and also maintains the required reservoir pressure. Gas injection, as part of secondary recovery, maintains the required reservoir pressure condition.

Tertiary or Enhanced Oil Recovery (EOR) processes are associated with the injection of a specific type of fluid or fluids into a reservoir. The injection of fluid supplements the natural energy left over in the reservoir and displaces the un-recovered oil. The increased interaction between the foreign fluid (injected fluid) and the in-place oil results in alterations in rock and fluid properties. Fluid injection and eventual interaction brings about changes like a lowering in interfacial tension (IFT), oil swelling, oil viscosity reduction, wettability modification, and sometimes favorable phase behavior conditions. These changes are mainly attributed to physics and the chemical interaction between the two

fluids and also to the rate and pressure with which these fluids are injected into the reservoir.

2.5.1. Miscible Displacement Processes (Green & Willhite, 1998)

Miscible displacement technique is one of the most popular enhanced oil recovery (EOR) methods practiced to recover oil from heavy immobile oil reservoirs. The miscible displacement process increases oil recovery by increasing the miscibility at the interface of displacing fluid and the displaced fluid (oil). This is primarily carried out by altering the composition of the immobile heavy oil such that any interaction with an injected fluid of a certain composition will bring about a single miscible phase between the two fluids. Hence, the composition of injected gas is carefully chosen so as to maintain complete miscibility with the in-place oil at all times.

Varieties of displacement fluids are used in the miscible recovery process. Some of the most commonly used fluids are CO_2, flue gas and nitrogen. Selection of these fluids depends primarily on availability. Economics also plays a vital role in deciding the level of enrichment.

Displacement fluids have been broadly classified under two categories. The first types are fluids that cause First Contact Miscibility (FCM causing fluids). Upon injection, these fluids form a single phase upon first contact when mixed in any proportion with the crude oil. The second type causes Multi Contact Miscibility (MCM causing fluids). Miscibility is achieved in situ through the compositional alteration of the crude oil and the injected gas as the displacing gas moves inside the reservoir and comes in contact with the oil several times.

Miscible displacement process substantially increases the microscopic displacement efficiency. Such high efficiency is not possible with waterflooding. Waterflooding successfully removes oil from big and medium sized throats but fails to push out trapped oil in the form of isolated drops, stringers, or perpendicular rings etc. This behavior is mainly attributed to the capillary forces. After achieving such conditions oil flow essentially drops to zero and any further injection produces a negligible amount of oil.

Miscible injection technique smartly tackles this problem. The displacing fluid first eliminates the interfacial tension between the in-place oil and itself and becomes a single phase system. The additional pressure produced by the injected fluid then provides additional energy to push the entire single phase out of the reservoir. The reduction in interfacial tension makes the trapped oil mobile and the additional pressure energy is high enough to mobilize trapped oil by overcoming the capillary forces, thereby increasing the overall recovery from the reservoir.

2.5.2. Gas Injection

Oil fields on the North Slope have always been the target of enhanced oil recovery applications. EOR is essential for the economic production of these extremely viscous oils. Waterflooding has been the most widely used method since the success of waterflood pilot project in 1983. Although it was successful, the results suggested a process would be needed that would yield a higher oil rate and recovery than waterflood alone. Naturally, since then efforts have been directed towards gas injection as an EOR technique. The abundance of gas streams on North Slope makes this an attractive option (DeRuiter et al., 1994).

DeRuiter et al. (1994) performed phase behavior experiments on West Sak oil. They investigated the solubility of methane, ethane, propane, n-butane and CO_2 in West Sak oil. Their detailed work included complete characterization of two oil samples from West Sak Reservoir (Upper & Lower West Sak interval). The property of the Lower West Sak interval (referred as Oil A in the report, Table 2.2) oil sample matches the type of oil chosen under the present study.

Table 2.2: Oil Properties

Oil	Molecular Weight	Viscosity at 75 °F	Density (g/cm3) at 60 °F
A	330	256	0.9433
B	446	5392	0.9725

Several static experiments were carried out by the team to estimate live viscosity, the live density of an oil sample under different pressure conditions. GOR was measured by flashing the live oil sample to atmospheric conditions. General properties like molecular weight and compositional analysis were also carried out. Followed by static experiments they estimated the Minimum Miscibility Pressure (MMP) and Minimum Miscibility Enrichment (MME) value by carrying out slim tube experiments. The confirmation of miscibility was assumed to happen when oil recovery was higher than 90% and with absence of gas spiking before breakthrough.

Thus, DeRuiter's work gives an insight into the phase behavior of West Sak Oil and guides in choosing the optimum conditions for performing miscible injection. The results of Lower West Sak interval oil has been summarized in following paragraphs.

Differential liberation tests were carried out using methane, CO_2 and ethane separately. Based on their observations they concluded the following for each case. With methane they concluded that with increase in saturation pressure for oil the GOR was increasing. They were able to match the experimental data with Standing's correlation quite closely. Live oil viscosity on the other hand exhibited substantial dependence on methane solubility. West Sak Oil showed approximately five times decrease in viscosity with increase in saturation pressure (increasing methane solubility) (Figure 2.2).

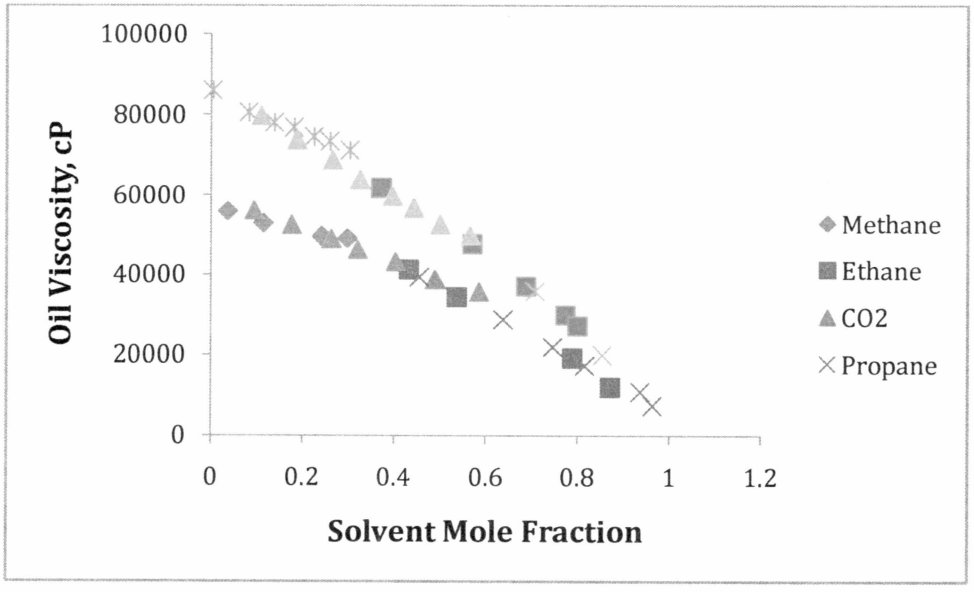

Figure 2.2: Viscosity behavior of West Sak oil (reproduced from DeRuiter et al., 1994)

Differential Liberation tests with CO_2 were of interest to this study. DeRuiter et al., in their efforts to characterize oil with CO_2, obtained some interesting results. Carbon dioxide solubility in oil showed an initial increase with saturation pressure

until the CO_2 liquefaction pressure was reached (approx 800 psi at 65 °F, Figure 2.3). Beyond that, CO_2 solubility remained constant. While estimating live density with CO_2 they concluded that CO_2 solubility (saturation pressure) and phase density increase almost linearly (Figure 2.4). Beyond CO_2 liquefaction pressure, the increase in live oil density was attributed mainly to an increase in overall system pressure.

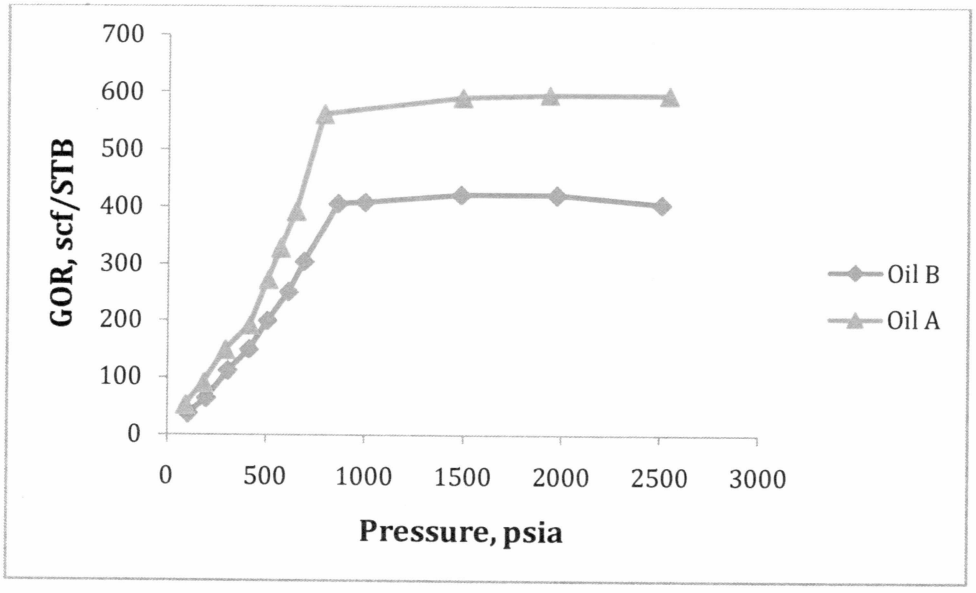

Figure 2.3: CO_2 solubility vs pressure (reproduced from DeRuiter et al., 1994)

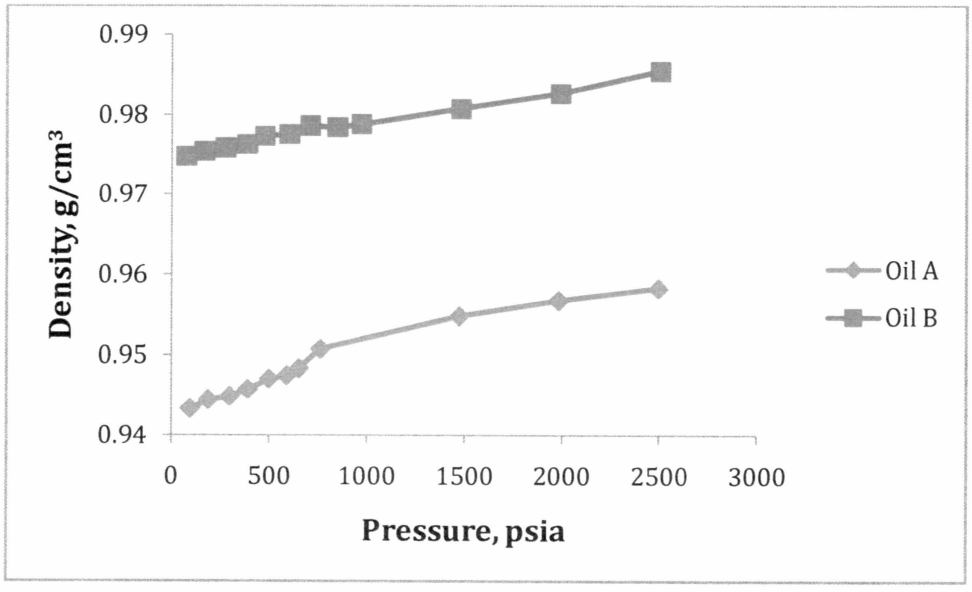

Figure 2.4: CO_2 saturated oil density (reproduced from DeRuiter et al., 1994)

Ethane behaved similarly to methane and CO_2, displaying an increase in solubility with saturation pressure increase. Beyond liquefaction pressure (580 psi), ethane showed a formation of a second upper liquid phase. With an increase in ethane concentration, this upper liquid phase expanded in volume. A significant amount of extracted oil was observed in this phase. However, with pressure around 1500 psi, ethane solubility experiments showed formation of a lower oil phase. This oil phase grew in size with an increase in ethane concentration. DeRuiter and team concluded that these phase developments were similar to bubble point and dew point conditions. They observed the growth of the lower oil phase to be equivalent to dew point behavior whereas the growth of the upper liquid phase was observed to be similar to bubble point behavior. Thus, with these observations, they inferred that the critical point exists between 580 psi and 1500 psi.

DeRuiter et al. (1994) carried out all displacement experiments with Oil A. Slim tube experiments were performed with pure CO_2 and oil at 2000 psi. With CO_2 in liquid state, despite high displacement pressure, recovery was very low, indicating an immiscible displacement. When several runs were carried with ethane, good recoveries were obtained, indicating the presence of miscible displacement. During these experiments, they also observed some extent of two phase flow, confirming that the miscibility was not First Contact Miscibility (FCM). In these experiments, MMP was interpreted to be at the ethane liquefaction pressure.

DeRuiter et al. (1994) thus concluded that ethane developed miscibility with West Sak oil while in its sub-critical liquid state. Miscibility was observed to be of the Multi Contact type and followed condensing-vaporizing mechanism. When using an enriched gas/lean gas combination they observed a transition from FCM to multi contact miscibility to immiscible behavior by increasing lean gas concentration. This transition was observed at enrichments of 42% methane. With further dilution up to 61%, the flow was immiscible but there was an increase in recovery. Recovery behaviors were observed to be unusual at high lean gas concentrations. This was mostly attributed to complex phase behavior of the oil-gas system (Figure 2.5).

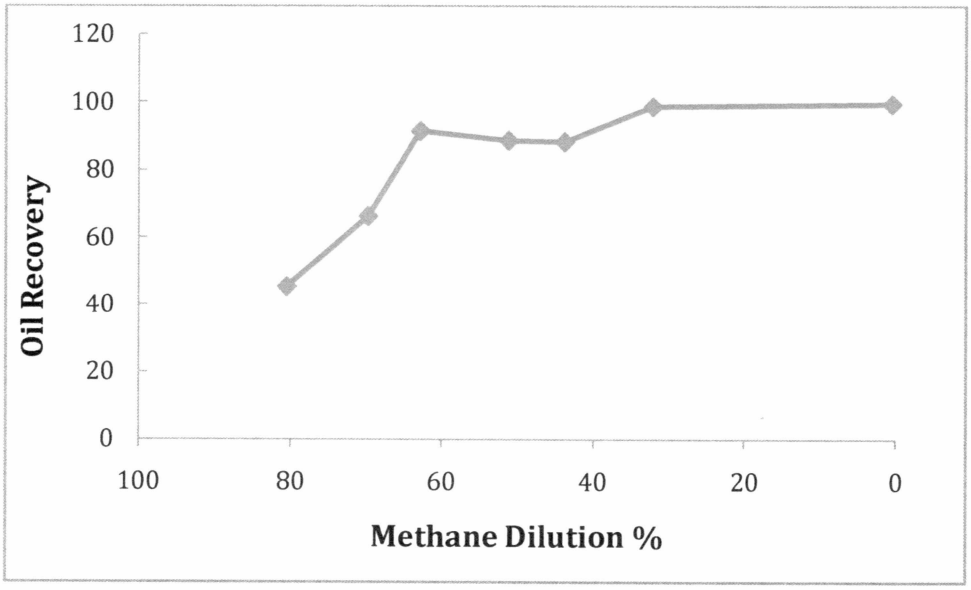

Figure 2.5: Oil recovery for various enrichment of the injectant gas (reproduced from DeRuiter et al., 1994)

Sharma et al. (1989) in their study of the miscible displacement of West Sak crude have also concluded that multi-contact miscibility can be developed for enriched gas drives by using a condensing-vaporizing mechanism.

2.6. Reservoir Simulation

The predictive capabilities of reservoir simulation software helps engineers design field scale projects. Miscible injection, as an alternative technique to other EOR techniques to enhance production, is dominated by compositional changes taking place due to mass-transfer between various phases. To model such a process, a compositional simulator is an ideal choice.

GEM is CMG's advanced general equation-of-state compositional simulator which includes options such as equation-of-state, dual porosity, CO_2, miscible gases,

volatile oil, gas condensate, horizontal wells, well management, complex phase behavior and many more. GEM was developed to simulate the compositional effects of reservoir fluid during primary and enhanced oil recovery processes. GEM is an efficient, multidimensional, EOS compositional simulator which can simulate all the important mechanisms of a miscible gas injection process, i.e. vaporization and swelling of oil, condensation of gas, viscosity and interfacial tension reduction, and the formation of a miscible solvent bank through multiple contacts.

Chapter 3

Methodology

3.1. Equation of State Model Development

The Peng-Robinson equation of state (PR EOS) was used for the study for the following reasons:

- The PR EOS uses a universal critical compressibility factor of 0.307, which is closer to the experimental values for heavier hydrocarbons and somewhat lower than the Redlich-Kwong value of 0.333.
- The PR EOS gives more accurate and satisfactory volumetric predictions for vapor and liquid phases when used with volume translation.

The experimental data which was used for carrying out the equation of state modeling consisted of the following:

- Compositional analysis of the West Sak oil up to C_{21+}
- Saturation pressure at the reservoir temperature of 80 °F
- Pressure-Volume-Temperature *(PVT)* experimental data mainly differential liberation (DL), constant composition expansion (CCE)

PVT experimental data was obtained from the previous studies carried out at University of Alaska Fairbanks (UAF) on the West Sak oil and is given in the Appendix A.

To study how well the data fits PR EOS, initial runs were carried out using just the compositional data. The shape of the phase envelope was studied along with the predicted saturation pressure. When it was found that the predictions were erroneous in the absence of tuning, experimental data was used to fit the

predicted values by regression of EOS parameters. The initial regression runs were carried out using the original West Sak oil composition distribution to narrow down the number of EOS parameters used for regression. Different EOS parameters were selected and regression was carried out until a good match between the experimental data and the values predicted by WinProp was obtained. Careful attention was paid to the number of data points used in the tuning. Too many data points would add to the complexity of regression and the flexibility of EOS parameters. Too few data points would not give good predictions. Likewise, oil viscosity, liquid volume %, and relative volume were selected as the experimental data set because it was found that it was difficult to get a good match of these date points. The main objective during such runs was obtaining a good match of saturation pressure values. Getting a good match of oil viscosities and oil densities was the main point of focus during subsequent runs. However, the predictions of other PVT properties were maintained within a reasonable range. Apart from changing the combination of EOS parameters selected for regression, different property correlations were also tried out. Likewise, viscosity models such as Jossi-Stiel-Thodos and Pedersen's Corresponding State model were studied for their predictions. The effect of the inclusion of binary interaction parameters (BIP) on the EOS predictions was also studied. The percent deviation in the values of EOS parameters used for tuning was maintained within a permissible range defined by the parameter itself and the regression model.

Once a good match between the experimental values and EOS predictions was obtained, lumping was carried out to reduce the number of components. Lumping reduces the time required for reservoir simulation. Different lumping

schemes were used and the results were studied. The main aim was to reduce the number of components as much as possible without compromising on the accuracy of EOS predictions. Step by step procedure adopted for EOS model development is listed in the Appendix B in the form of a flowchart.

The same procedure used for characterized oil sample was adopted to tune the EOS for the lumped sample. Finally, we had a tuned EOS with the lumped sample, which was used in CMG GEM (discussed in Section 3.2) for reservoir simulation purposes.

3.2. Reservoir Simulation

After developing the model for EOS, the next task was to study the potential of the West Sak reservoir for enhanced oil recovery (EOR) using gas injection. As West Sak is a very huge reservoir, for simulation purposes a 40 acre area was chosen. Initially a comparative study was performed for different gases to be used as the injectant for enhanced oil recovery. A vertical 5-spot injection pattern was selected with the four injectors at the four corners and a producer well at the center. The project life was 25 years, from Jan 2006 to Dec 2030. After a detailed analysis for this vertical injection pattern was performed, the gas with the best performance was selected for study of its effectiveness in a horizontal well pattern case.

CMG's GEM, a reservoir simulation application was used for the study. GEM provides features such as the building of grid blocks to define the reservoir and its properties (porosity, permeability, sand layer thickness, depth, water saturation, relative permeability). Operating conditions such as the temperature and pressure can also be defined. Reservoir performance under various operating parameters

such as the well bottom-hole pressure and production rates of oil and gas, can be analyzed.

3.2.1. Model Development

To define the reservoir, a three dimensional Cartesian co-ordinate system was used for the study. Accordingly, I, J, and K defined the three directional axes; I and J axes perpendicular to each other and in the same plane, and K axis was perpendicular to the IJ plane. The West Sak reservoir was defined to have five producing layers with definite porosity and permeability values, with alternate shale layers embedded in between the sand layers. The shale layer was considered to be impermeable with zero porosity. The entire reservoir was built in the form of grid blocks in all the three directions. Accordingly, for a 40 acre area, there were 25 grid blocks each in the I and J direction and 9 such planes of grid blocks in the K direction making a total of 5625 grid blocks for the entire reservoir. A pictorial view of the reservoir configuration with marked locations of producer and injectors is shown in Figure 3.1. The reservoir properties are listed in Table 3.1

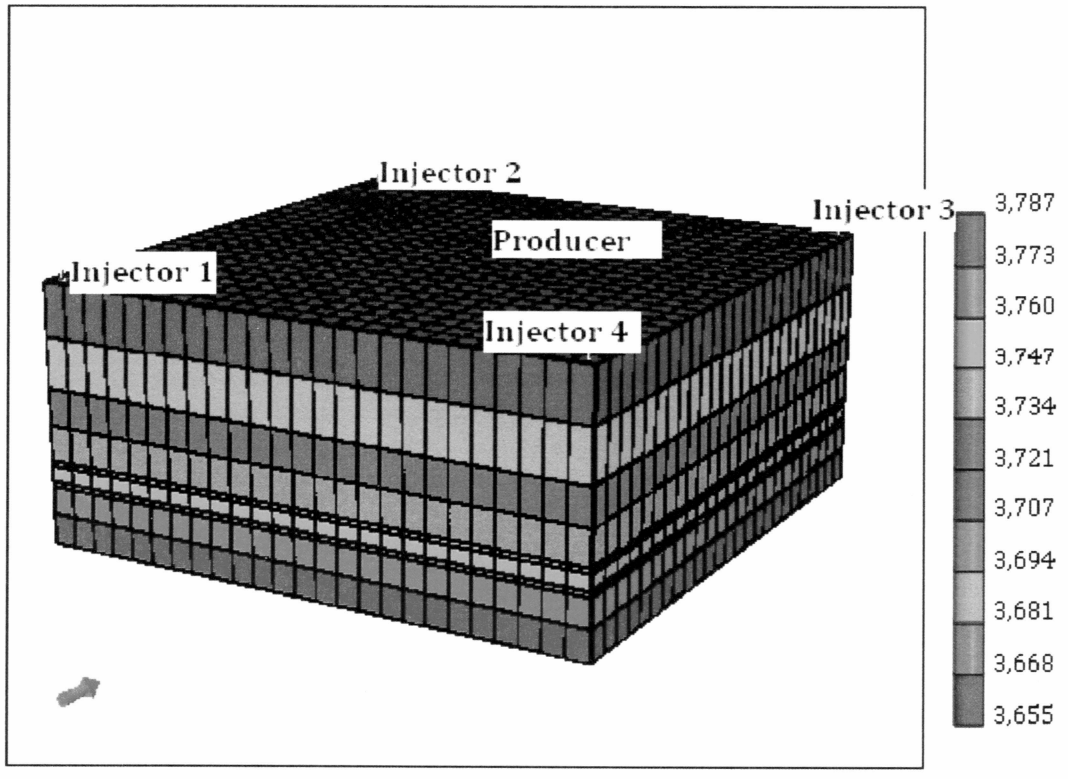

Figure 3.1: West Sak reservoir model view

Table 3.1: West Sak reservoir properties (Bakshi, 1992)

Layer No.	Sand	Interval (ft)	Avg. Porosity (%)	Avg. water saturation, (%)	Net pay (ft)
9-topmost	Upper 1	3544-3584	30	24	30
7	Upper 2	3614-3640	31	31	21
5	Lower 1	3660-3686	23	45	3
3	Lower 2	3695-3760	25	47	3
1-bottommost	Lower3	3776-3814	27	41	17

Relative permeability data required for the model development was taken from Bakshi (1991) and is shown in the form of following relative permeability plots (Figure 3.2 to Figure 3.7).

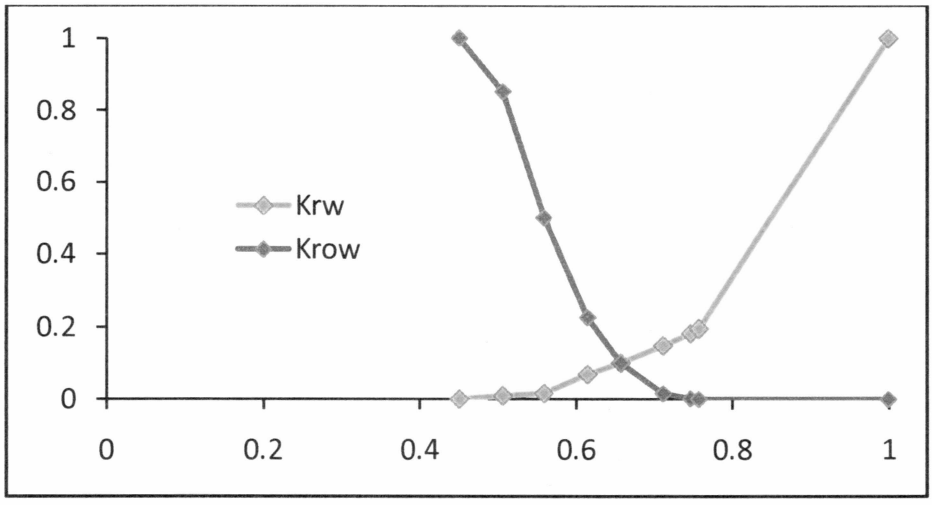

Figure 3.2: Water Oil relative permeability of West Sak upper sand # 1 (Bakshi, 1991)

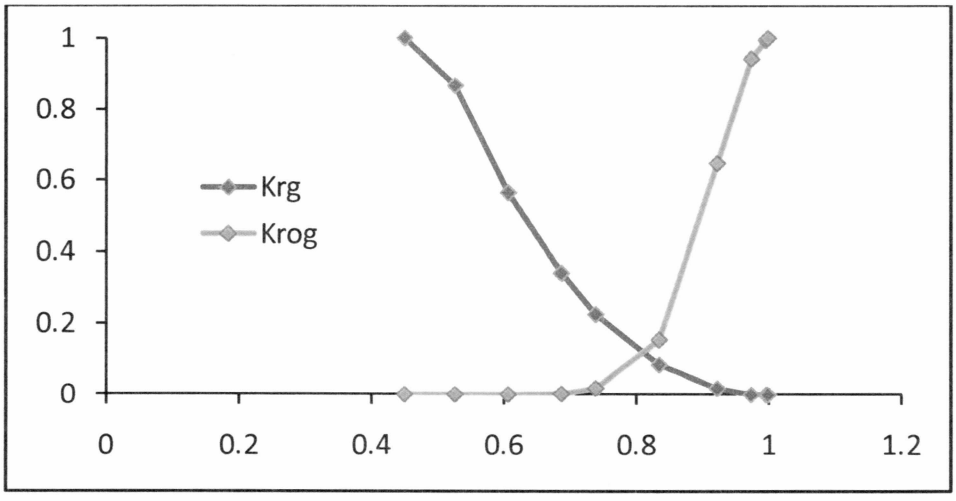

Figure 3.3: Gas Oil relative permeability of West Sak upper sand # 1 (Bakshi, 1991)

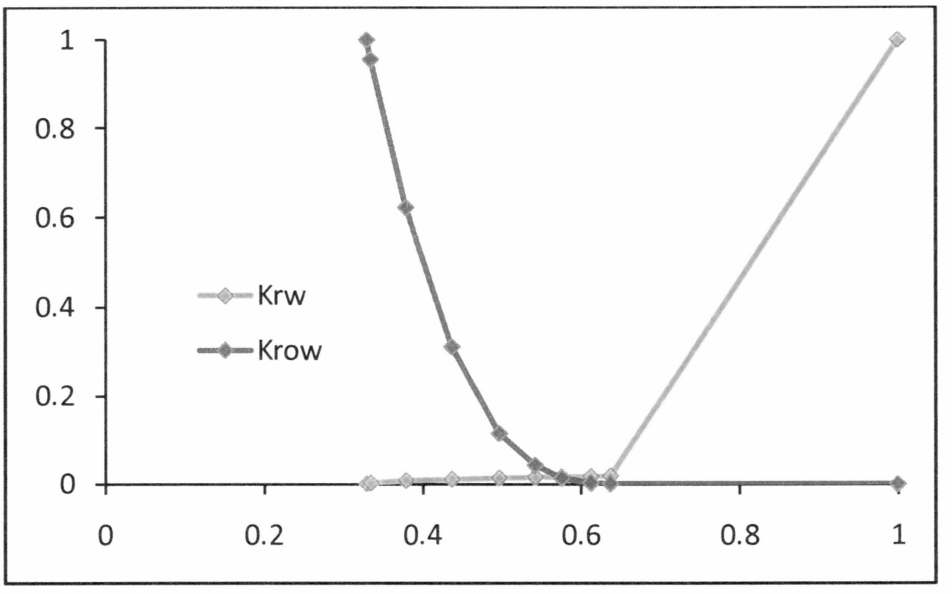

Figure 3.4: Water Oil relative permeability of West Sak upper sand # 2 (Bakshi, 1991)

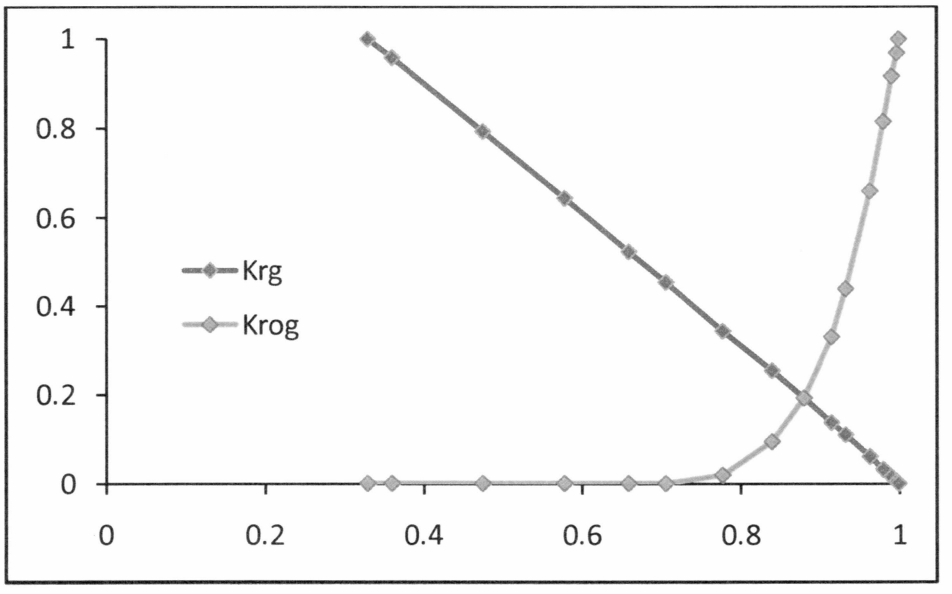

Figure 3.5: Gas Oil relative permeability of West Sak upper sand # 2 (Bakshi, 1991)

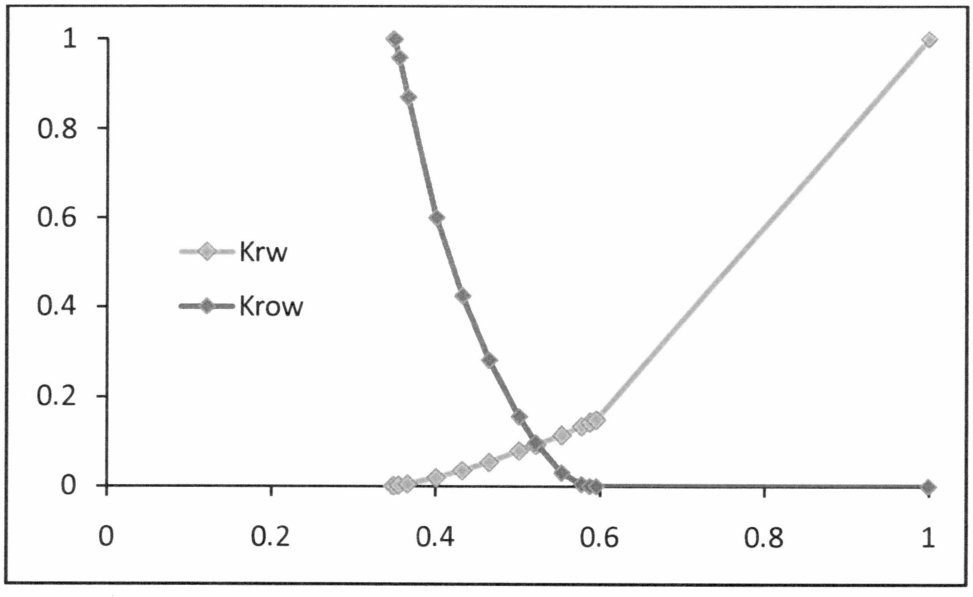

Figure 3.6: Water oil relative permeability of West Sak lower sands (Bakshi, 1991)

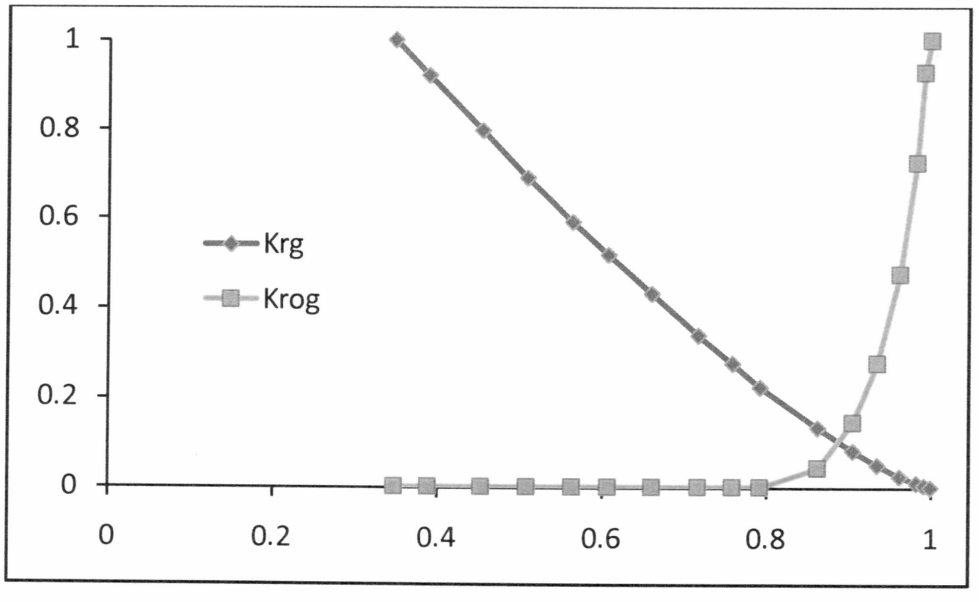

Figure 3.7: Gas oil relative permeability of West Sak lower sands (Bakshi, 1991)

3.2.2. Enhanced Oil Recovery

After building the reservoir model using CMG's GEM, reservoir simulation studies of enhanced oil recovery for the West Sak reservoir using gas injection were carried out. The first task was the selection of gases to be used as injectant in the study. Since this was intended to be a comparative study, gases covering a wide spectrum of compositional variations were considered. The basic requirement for such a selection was the availability of the gases on the North Slope. (Patil, 2006) has proposed geologic sequestration of CO_2 as an option to control its emissions on the North Slope. This sequestered CO_2 can be utilized as an injectant in EOR. Sharma et al. (1988) estimated the Prudhoe Bay field to contain approximately 29 trillion cubic feet of natural gas, composed mainly of methane. Such a large reservoir of gas can definitely serve as the source gas in any gas injection scheme. MI 1, MI 8 and West Sak VRI are the gases currently used as injectant gases by BP Exploration (Alaska) Inc. (BPXA) on the ANS under various EOR schemes. All these gases were employed for EOR after careful study of the reservoir and the conditions present. West Sak VRI is one such gas designed by BPXA for the West Sak reservoir. VRI simply stands for viscosity reducing injectant and is manufactured by mixing heavy components with the produced gas which is generally lean on the North Slope. Some amount of CO_2 stripping is required to achieve miscibility conditions. MI 8 was another such gas used on the North Slope. It is an extremely rich gas stripped completely of the heavier fractions (C_{7+}) and CO_2. It has 42% of intermediates mainly rich in C_3 and C_4. MI 1 is a very lean gas having almost 95% of methane.

Figure 3.8 provides a quick comparison of the compositional variation of the gases selected for the present study. The detailed compositional analysis is given in the Appendix A.

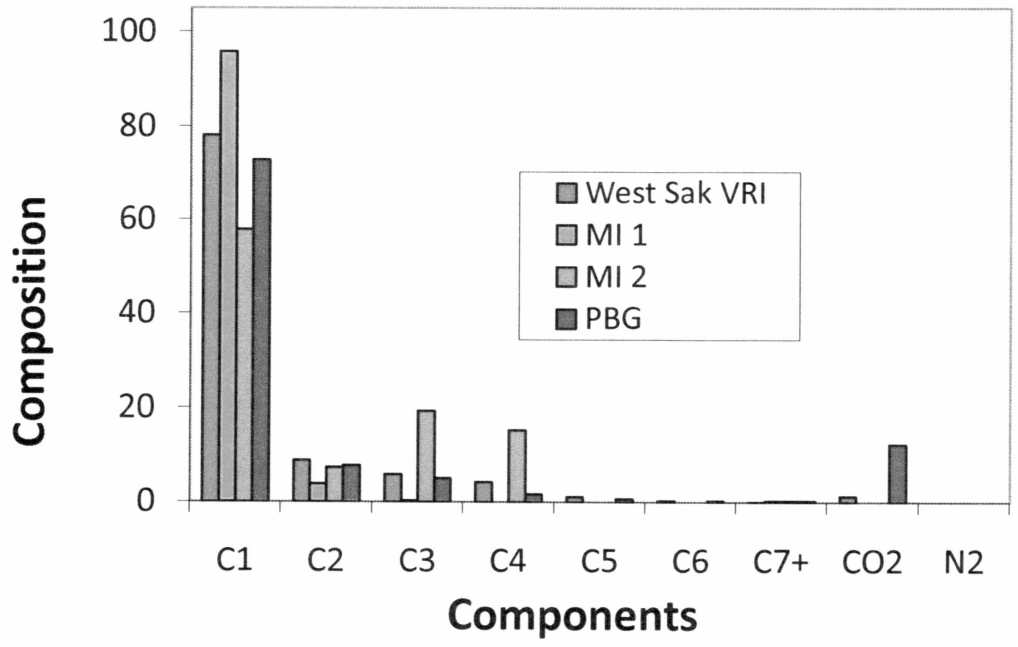

Figure 3.8: Component distribution comparison for the gas injectants

Having carefully selected the gases for the EOR study, the next step was designing the project. Project life was chosen to be for a period of 25 years. Necessary PV calculations were done and it was decided to use 10%, 20%, 30%, 40% and 50% as injection PV for different runs. Reservoir operating parameters are of prime importance in any reservoir simulation model. A due consideration to the integrity of these parameters should be given while making this selection. An obvious choice was to select bottom-hole pressure and production rate as the operating parameters. The values of these parameters were fixed after giving due

considerations to all the constraints. Some of these considerations were reservoir pressure, reservoir fracture pressure, draw-down, and daily production rates. Accordingly, bottom-hole pressure was set at 1400 psi and the production rate at 500 bbl/day. These operating parameters were kept fixed for all the gases and all the PV runs to make a uniform comparison. Gas injection pressure for the injector well was determined by the reservoir fracture pressure constraint and it was set at a value of 3000 psi. Gas injection are gets fixed depending upon the PV of gas being injected. A Vertical 5-spot injection pattern was chosen as shown in Figure 3.9.

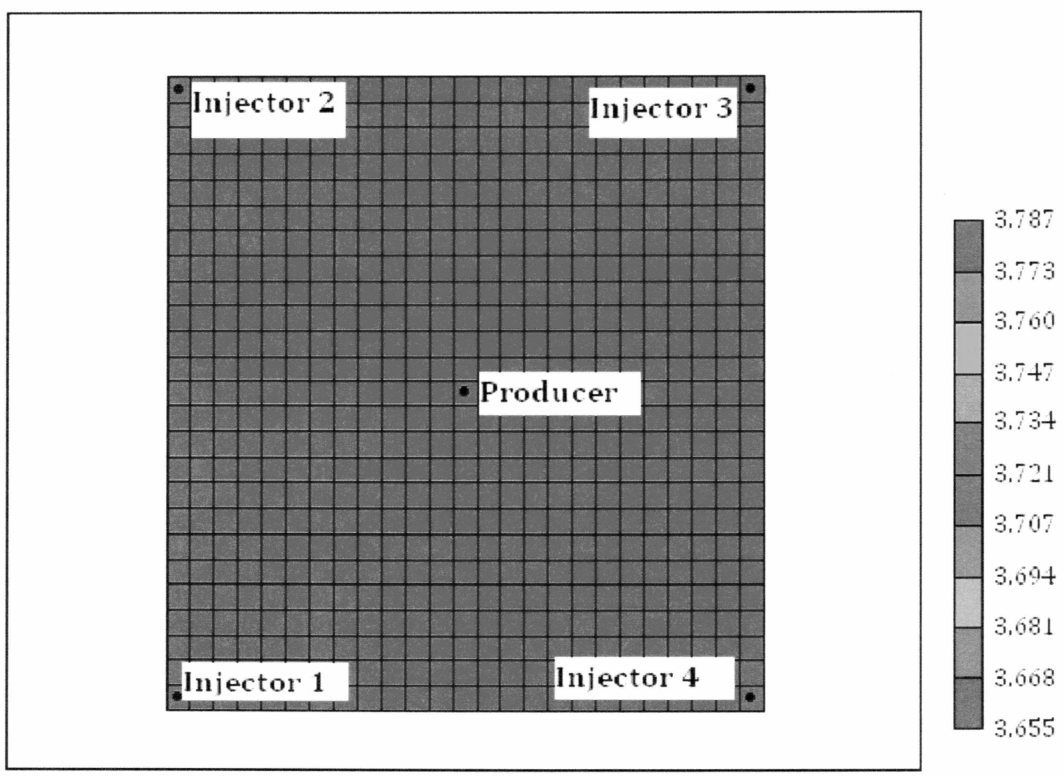

Figure 3.9: Top view of the reservoir model showing the location of producer and injector wells for a 5-spot injection pattern

To compare the potential of different gases as an EOR agents, we compared the production profiles for the entire life of the project for all the gases at different PV's. A simplistic comparison would be just to compare the cumulative recovery calculated in terms of original oil in place for all individual cases.

Plots of percentage pore volume of gas injected versus production rate were drawn to study the results. For the purpose of the comparative analysis of the performance of various gases, percentage pore volume of gas injected versus cumulative recovery was plotted.

After careful evaluation of results for a vertical five-spot injection pattern, simulation runs were drawn to study the performance of the West Sak reservoir for a horizontal producer with a horizontal injector case. Accordingly, two producers and two injectors were placed alternately (Figure 3.10 and Figure 3.11). Only three producing layers out of a total of five were perforated. This was because the remaining two layers were too thin to drill a horizontal well. The gas which performed the best in the case of vertical five-spot injection pattern was chosen as the injectant gas for the horizontal case. Accordingly, MI 8 was used. The same scheme of injection runs was employed for the horizontal case. Likewise, 10%, 20%, 30%, 40% PV injection runs were carried out. Reservoir operating parameters were optimized. It was found that using a BHP of 1400 psi, which was used for the vertical injection case, the gas breaks through very quickly. It was inferred that in the case of the horizontal injector, since the gas has much larger space to expand, it expands quickly. Hence the drawdown of 300 psi is too large for this case. After numerous runs, the well bottom-hole pressure was optimized at 1650 psi. Conditions for the injector wells were maintained at 3000

psi of injection pressure. Similar plots as those made for the vertical well case were made for horizontal injection to study the behavior. Accordingly, cumulative oil produced was plotted against time.

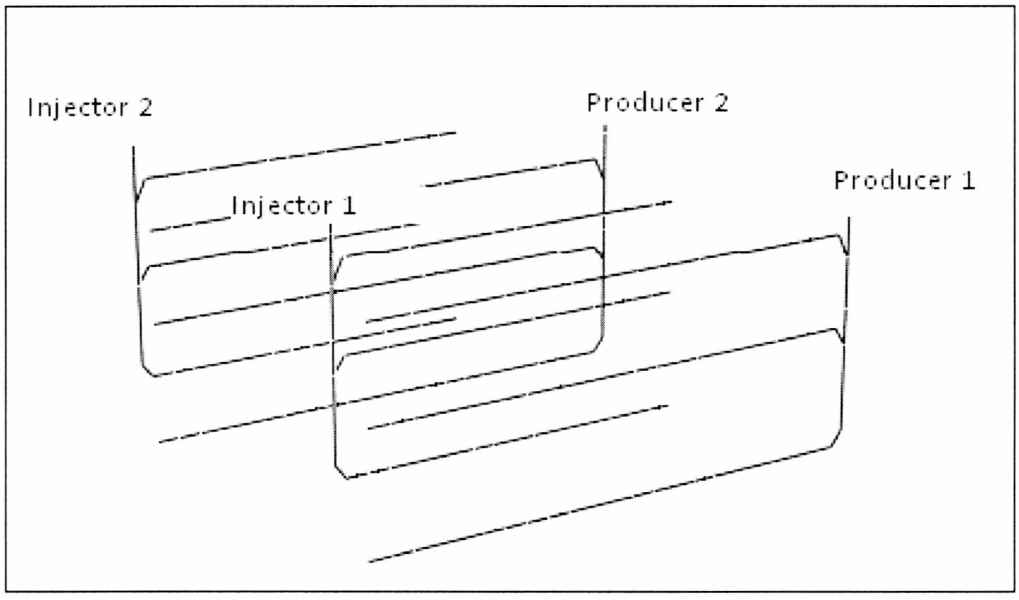

Figure 3.10: Three-dimensional pictorial representation of West Sak reservoir with alternate horizontal and producer wells

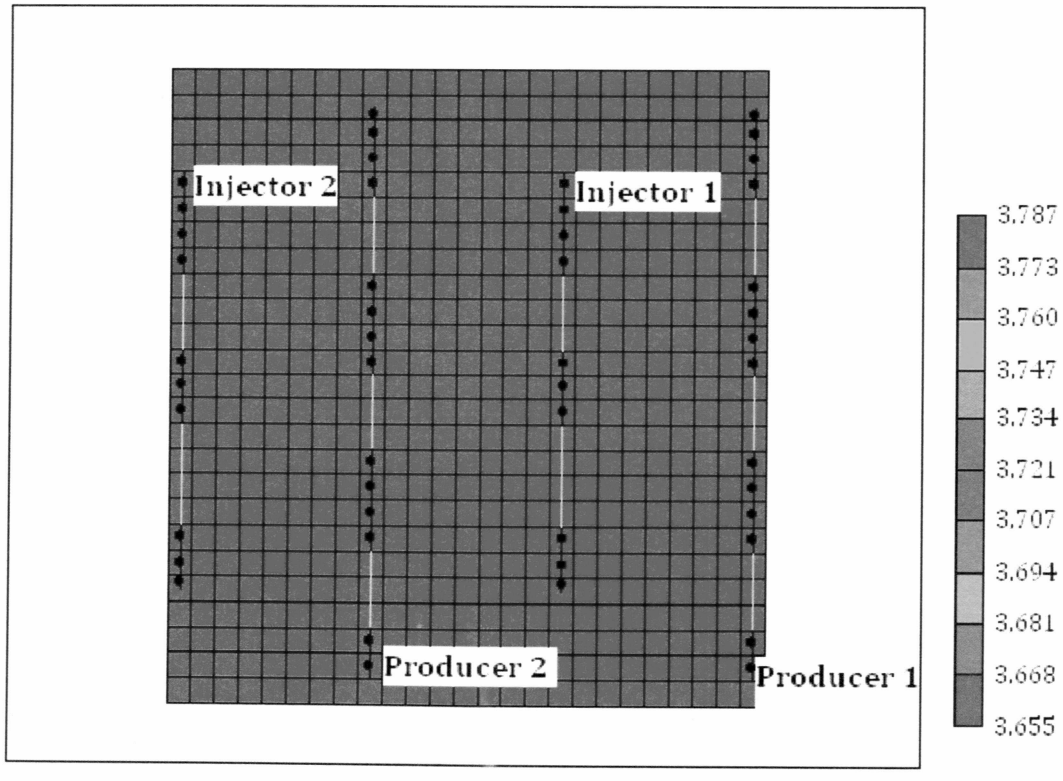

Figure 3.11: Top view of the reservoir model with the producers and injectors

Chapter 4

Results and Discussions

4.1. Equation of State

The performance of the untuned equation of state in predicting the phase envelope and the saturation pressure of the West Sak oil is given by Figure 4.1.

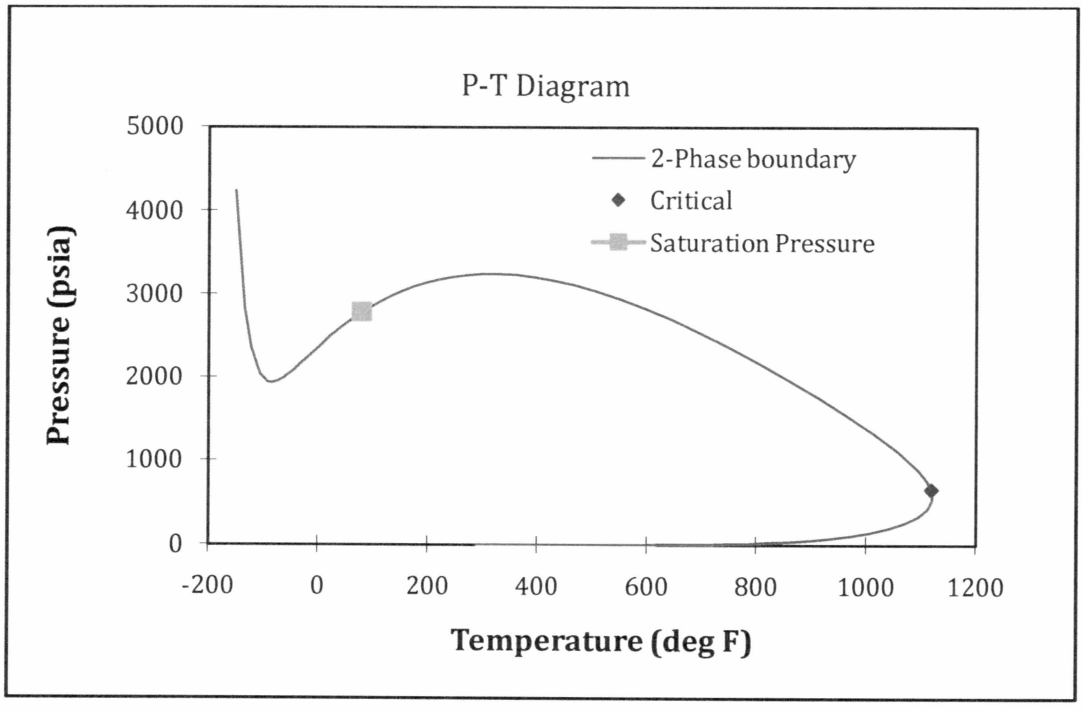

Figure 4.1: Phase envelope generated by the untuned EOS

The saturation pressure value for the West Sak oil predicted by the untuned equation of state was 2783.869 psia at the reservoir temperature of 80 °F. The experimental value was 1704 psia. The percentage difference in the two values was 63.37%, indicating a significant error in the prediction of saturation pressure.

The phase envelope (Figure 4.1) is also indicative of the erroneous predictions of the untuned EOS.

The EOS was hence tuned using CMG WINPROP. The tuning process improved the prediction of saturation pressure value and the value obtained was 1702 psia which was much closer to the experimental value of 1704 psia. The improvement in the phase behavior predictions can be seen from the phase envelope generated by the tuned EOS (Figure 4.2).

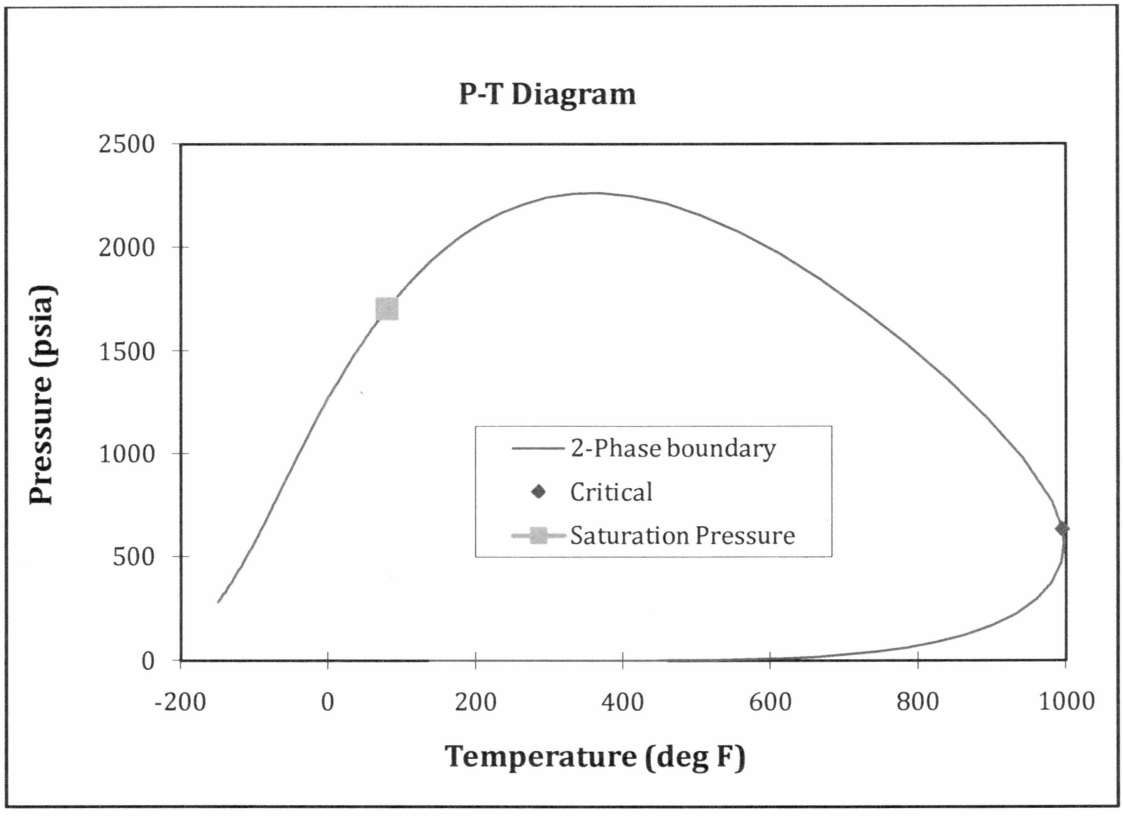

Figure 4.2: Phase envelope after tuning the EOS

Regression Scheme

Splitting of the C_{21+} fraction was first done up to C_{45+}. The gamma probability distribution function was used as the splitting model. The critical properties of the components after splitting were calculated using the Twu correlation. Lumping of components was then carried out. Accordingly, components heavier than C_7 were lumped together into a single component fraction as C_{7+}. This plus fraction had components from C_7 to C_{21+}. Lumping was done to reduce the simulation time in the reservoir simulator. The component compositions and properties after lumping are given below in Table 4.1.

Table 4.1: Composition and physical property data for the lumped components

Components	Composition	P_c atm	T_c K	Acentric Factor	Mol. Wt.
C02	0.0001597	72.8	304.2	0.225	44.01
N2	0.0003194	33.5	126.2	0.04	28.013
C1	0.3826031	45.4	190.6	0.008	16.043
C2	0.0085537	48.2	305.4	0.098	30.07
C3	0.0035832	41.9	369.8	0.152	44.097
NC4	0.0017866	37.5	425.2	0.193	58.124
NC4	0.0006388	33.3	469.6	0.251	72.151
FC6	0.0019962	32.46	507.5	0.275	86
C7+	0.6003593	12.269	889.54	0.961	368.85

This lumped data series was used for further tuning of EOS. For the purpose of tuning, several experimental data points were selected and given a weight. This weight scheme acts as the guideline for the regression model signifying the importance of that particular data point. The more the weightage given to a particular data point, the more forcibly the model will try to fit it. Since the top most priority of any tuning scheme is first achieving a very good match of the saturation pressure, it is always given the highest weightage. But in this case, the liquid density was found to be very difficult to match and was hence assigned the highest weightage. The experimental data points selected and the weightage given to them are tabulated below in Table 4.2.

Table 4.2: Weight distribution for EOS parameters

Data Point	**Weightage**
Saturation Pressure	30
Liquid Density	50
Oil Specific Gravity SG	50
Relative Oil Volume	1
Liquid Volume %	1

The next task was the selection of parameters to be used for regression. The following parameters were finally selected.

1. Critical Pressure of C_{7+} (P_C)
2. Critical Temperature of C_{7+} (T_C)
3. Acentric Factor of C_{7+} (AF)

4. Volume Shift (SH)
5. Coefficients of Pedersen's corresponding states viscosity model
    a. MW mixing rule coefficient (MU1)
    b. MW mixing rule exponent (MU2)
    c. Coupling factor correlation coefficient (MU3)
    d. Coupling factor correlation density exponent (MU4)
    e. Coupling factor correlation MW exponent (MU5)

The percentile changes in the values of these parameters during regression are given below in Table 4.3

Table 4.3: Percentage changes in values of EOS parameters selected for regression

Variable	Initial Value	Final Value	% Change
P_C	12.269	12.1	-1.37
T_C	889.54	823.04	-7.48
AF	0.961	0.63607	-33.81
SH	0.11515	0.16844	46.29
MU1	0.00013	0.00016	22.7
MU2	2.303	2.4263	5.35
MU3	0.00738	0.00885	20
MU4	1.847	1.4776	-20
MU5	0.5173	0.55698	7.67

The performance of tuned and untuned EOS in matching different PVT properties like the oil viscosity, relative volume, and liquid volume %, is ascertained with the help of composite plots showing direct comparisons between the values before and after regression. Following plots (Figure 4.3 to Figure 4.5) show such comparisons clearly indicating a better match of the experimental values by the EOS after tuning. It is seen that the values obtained after regression (tuned EOS) exactly matches with the experimental values. In the absence of any tuning, it is seen that values before regression (untuned EOS) do not match with the experimental values. EOS predicted values at higher and lower pressures show a good match with the experimental values. The values at moderate pressures (1000 psia to 2000 psia) show much deviation from the experimental values. Since these pressures fall within our current operating range, they should be matched accurately.

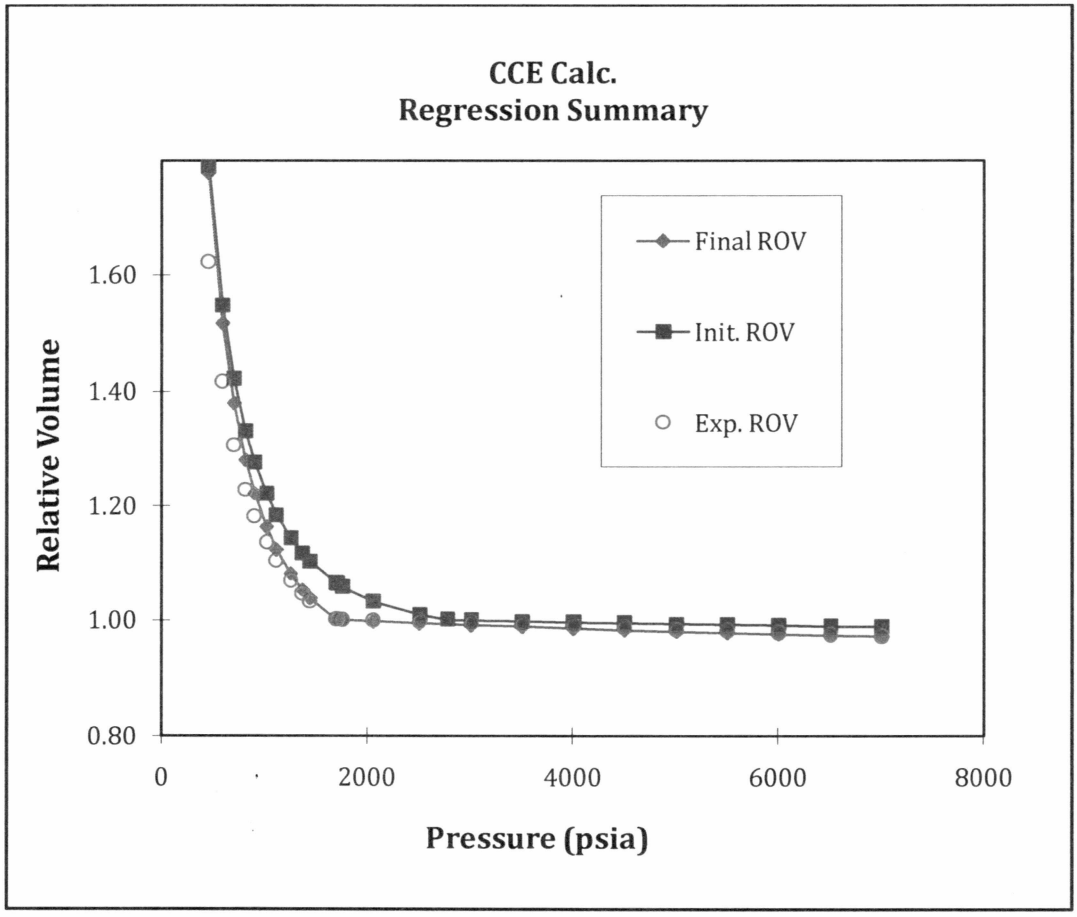

Figure 4.3: Regression summary for relative volume

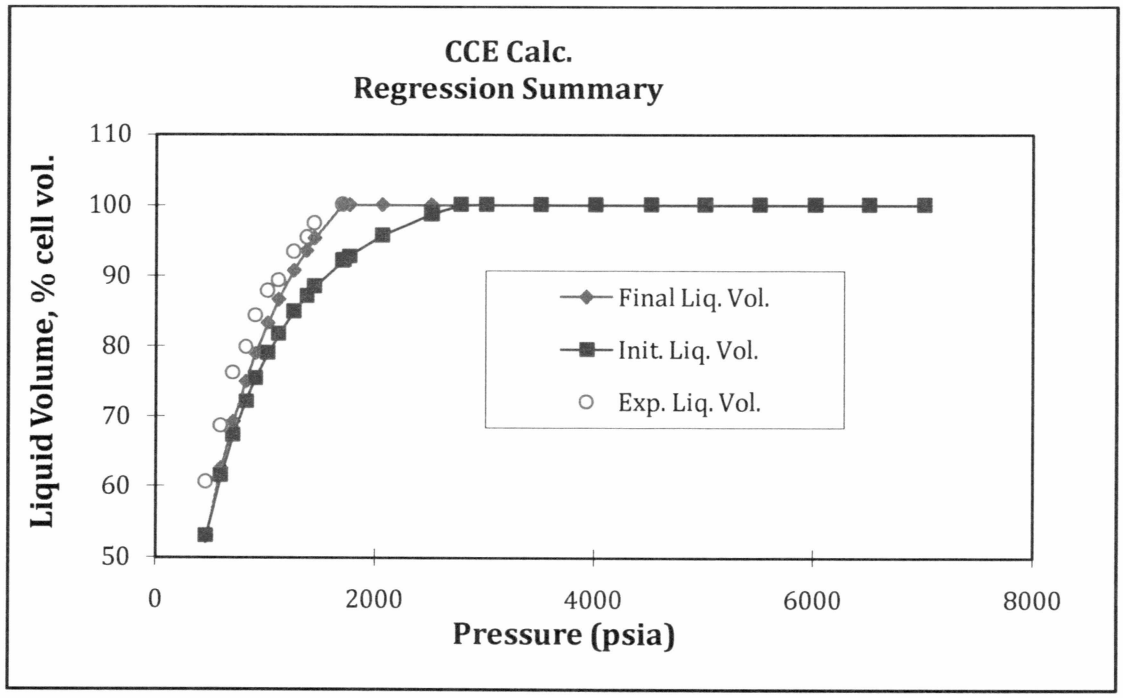

Figure 4.4: Regression summary for liquid volume %

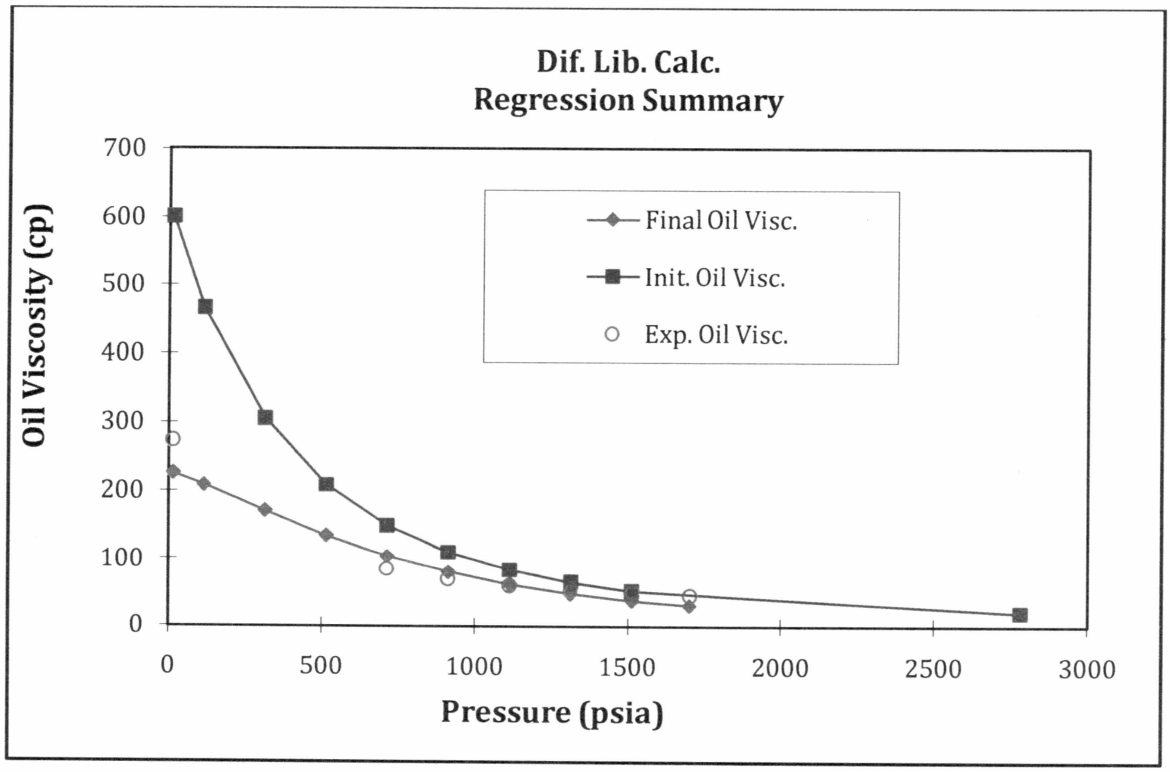

Figure 4.5: Regression summary for oil viscosity

After the tuning of EOS was successfully achieved, the consistency of the tuned EOS was verified. This was done by comparing the predicted values of the tuned EOS with the experimental data not used for tuning purposes. Gas formation volume factor (FVF), deviation factor z, and solution gas oil ratio (GOR) were such experimental data sets not used for in the tuning operation. The success of the tuned EOS will depend upon how well it predicts the values of these properties. Figure 4.6 to Figure 4.8 are the plots showing comparisons between the experimental data set and tuned EOS. There is a good match between the EOS predicted values and experimental values.

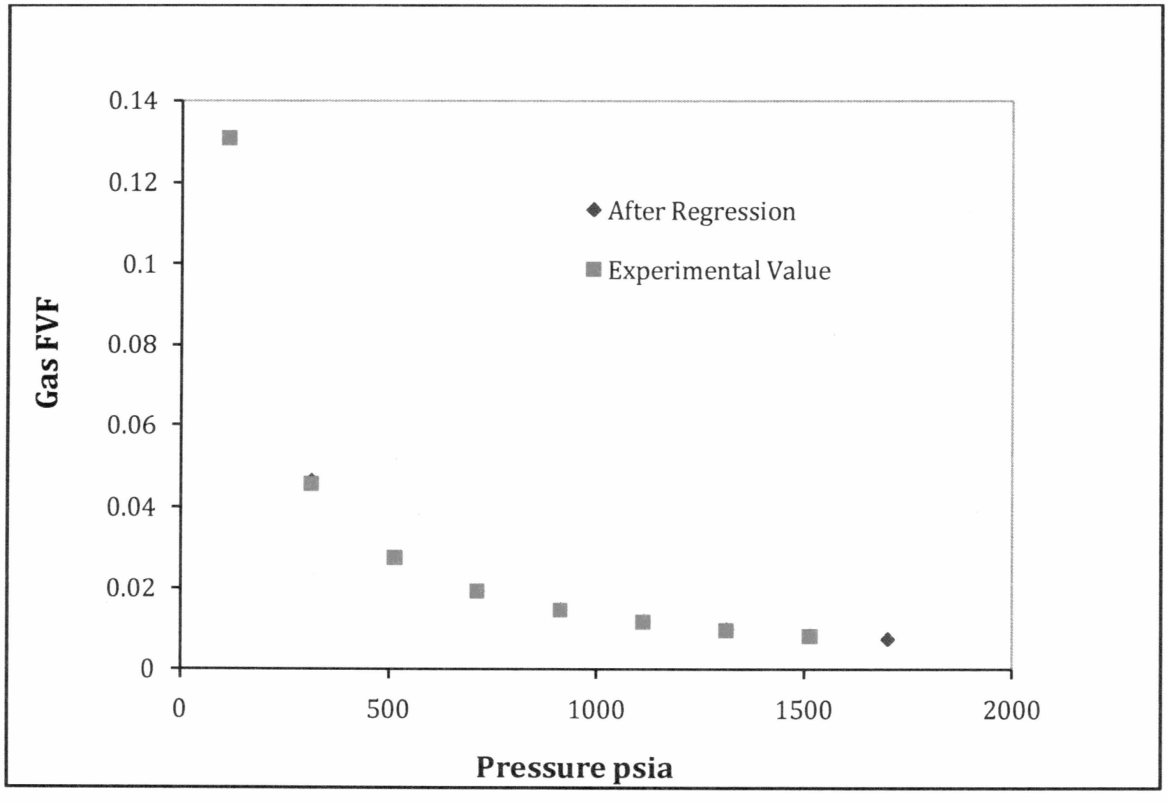

Figure 4.6: Experimental and EOS predicted values for gas FVF

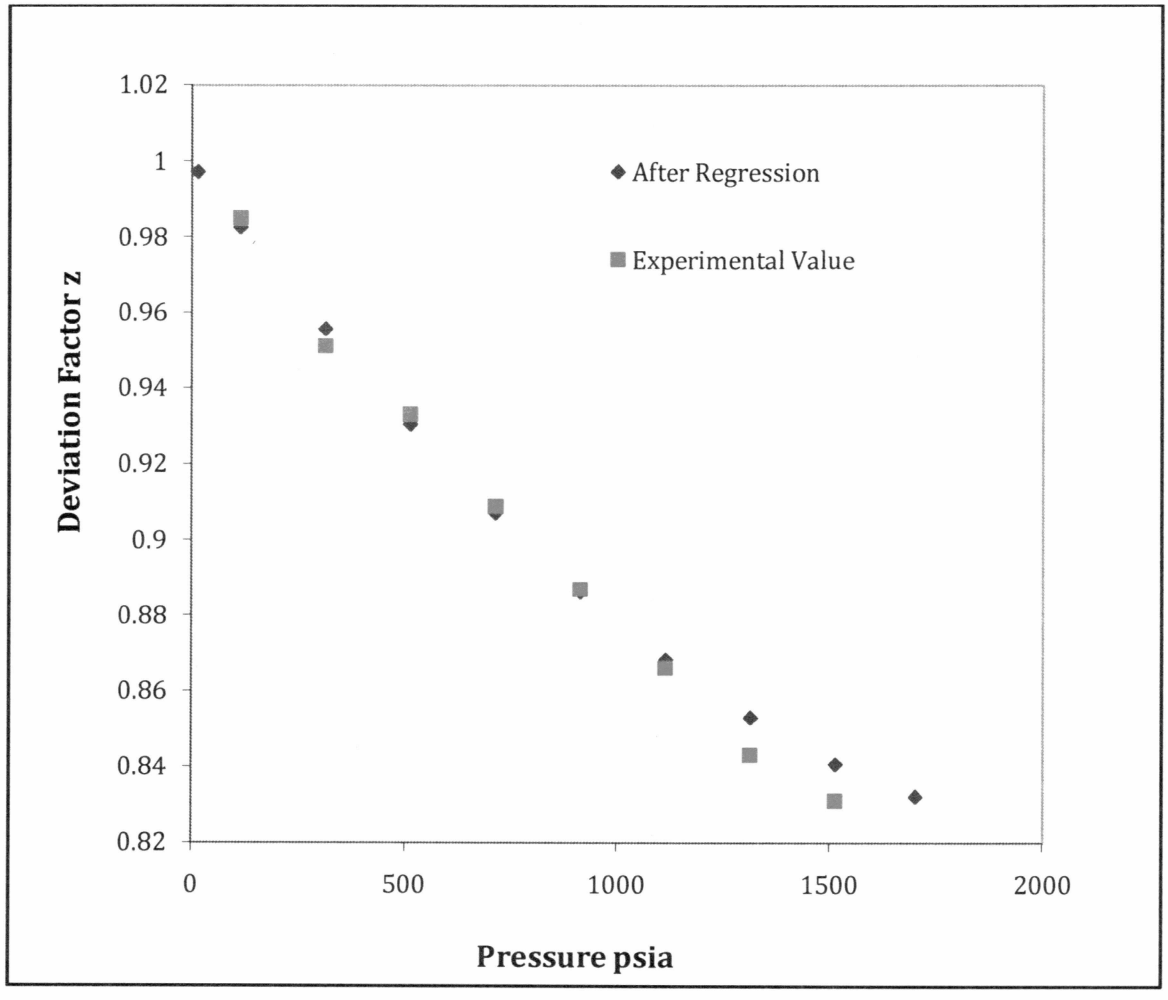

Figure 4.7: Experimental and EOS predicted values for deviation factor z

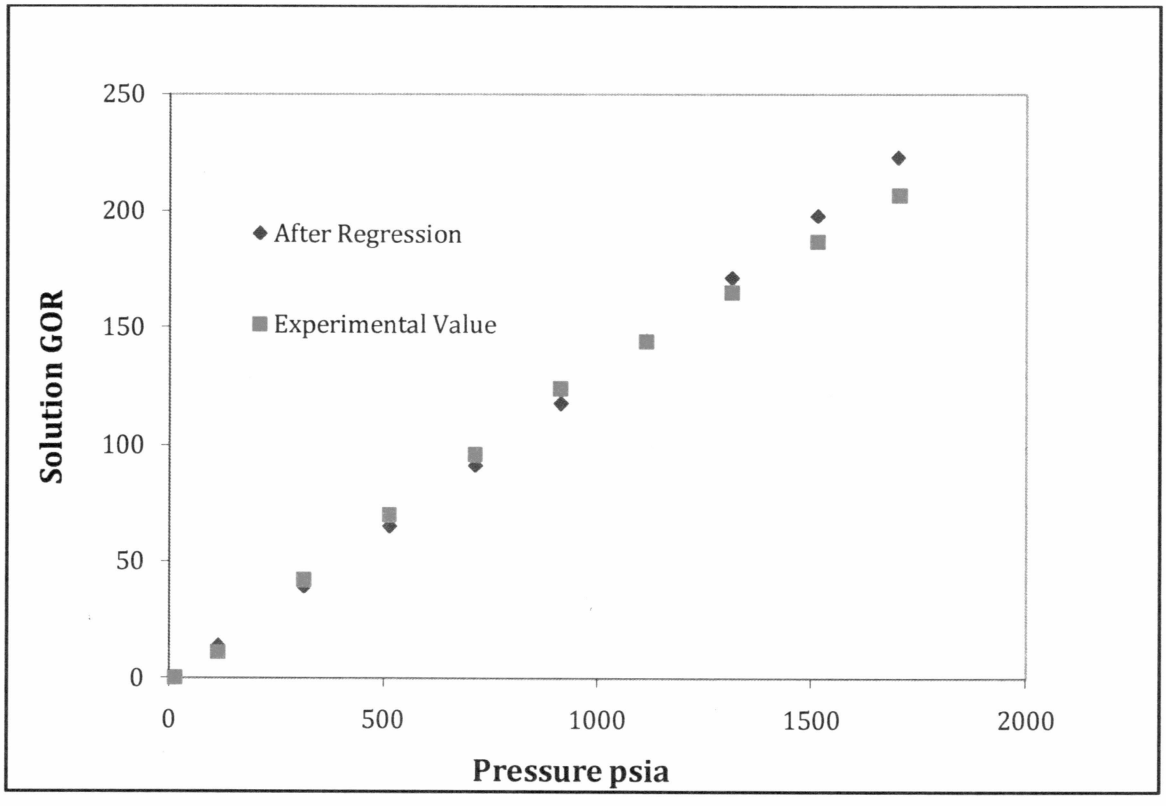

Figure 4.8: Experimental and EOS predicted values for solution GOR

4.2. Reservoir Simulation

4.2.1. Vertical five-spot injection pattern

Reservoir simulation to study the potential of EOR using gas injection was carried out next. Accordingly, 10%, 20,%, 30%, 40%, and 50% PV injection runs for all the injection gases were done. To make a comparative analysis, composite plots of cumulative oil produced and cumulative recovery obtained versus time were plotted for different pore volume injection runs and for all injection gases used in the study. MI 8, which is a rich gas, showed the best performance in terms of percentage recovery obtained and breakthrough achieved (Figure 4.9 & Figure 4.10). The onset of breakthrough can be determined by observing the cumulative production plots. It is observed that the occurrence of breakthrough is delayed

for lower PV injection of the injectant. Hence, for a 50% PV injection the breakthrough occurred after 11.5 years and for a 20% PV injection it occurred after 21.5 years (Figure 4.9 & Figure 4.10). Thus a decreasing trend is observed in the occurrence of breakthrough with increase in PV of gas being injected. But the cumulative recoveries shows a positive trend, increasing with the increase in PV of gas being injected. The recoveries achieved with MI 8 are as high as 44% for a 50% PV injection run (Figure 4.10). Daily production plots for rich gas injection are also plotted (Figure 4.11). They help us study the production profile along the life of project. As it can be seen that production rate increases until breakthrough and decreases after that which is usually the case for any injection case. The fluctuations that can be observed in these plots should not be confused with phenomenon of viscous fingering or phase trapping. These fluctuations simply indicate the numerical instability of the model. The model tries to satisfy two operating constraints (BHP and production rate) and when it reaches the limit of one of the operating constraint it switches on to another. This results in numerical instability.

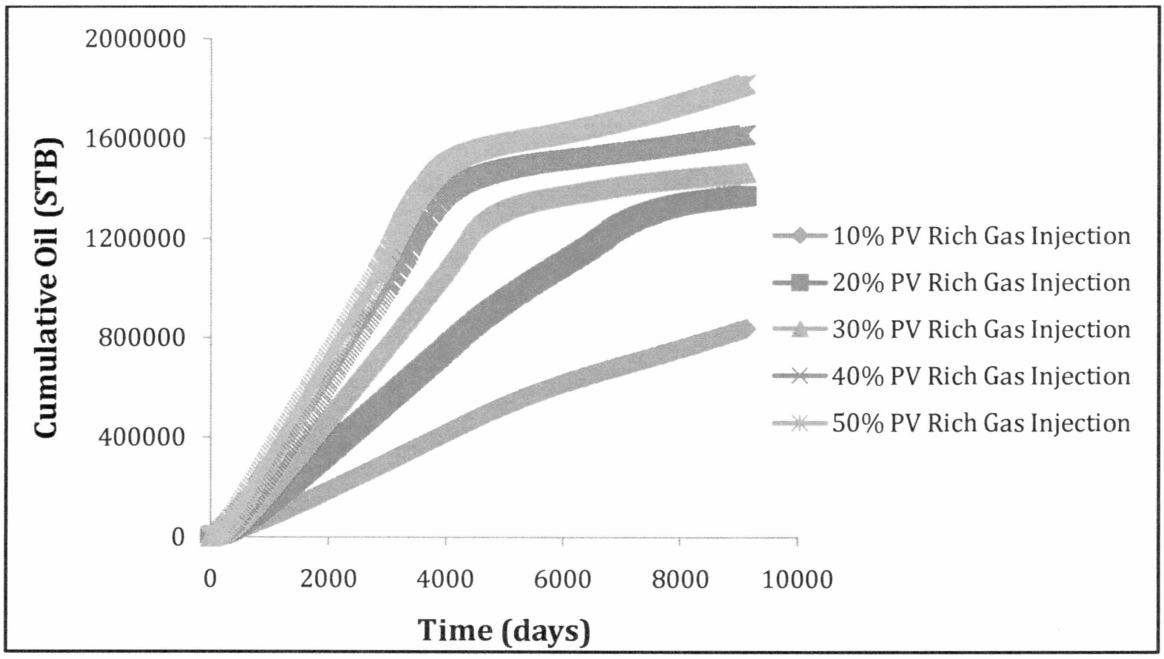

Figure 4.9: Composite cumulative oil produced plot for rich gas injection

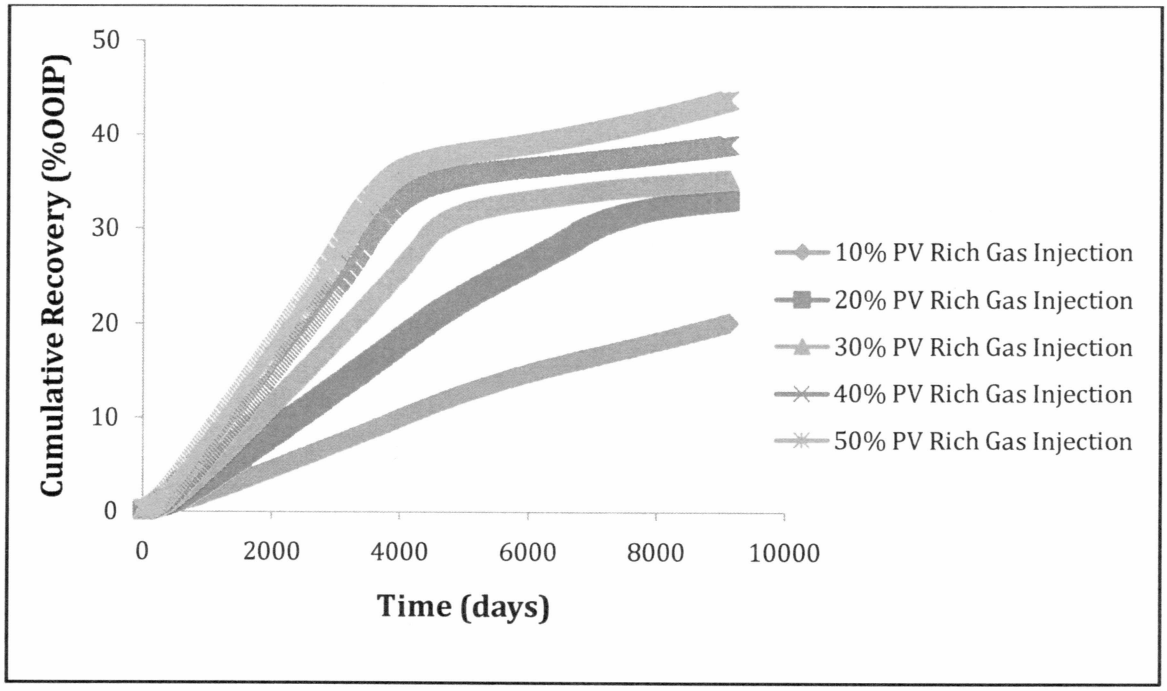

Figure 4.10: Composite cumulative oil recovery plot for rich gas injection

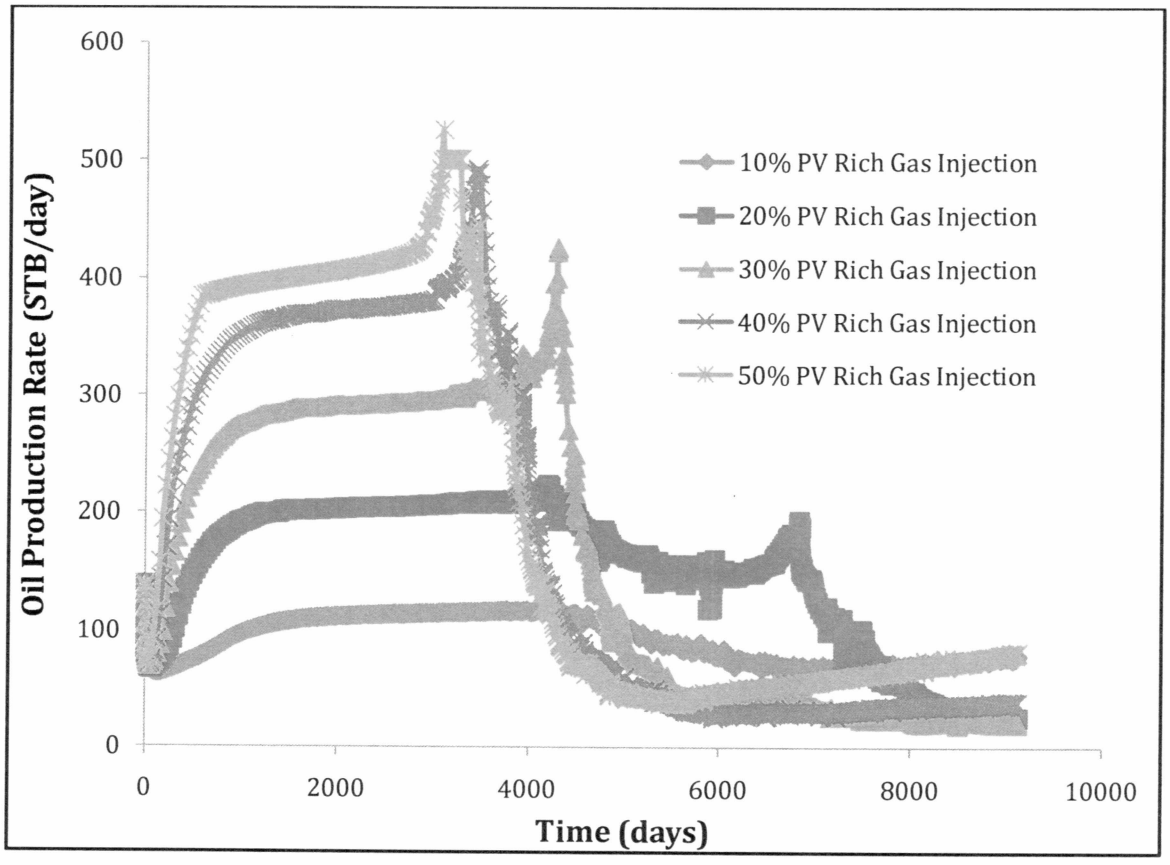

Figure 4.11: Composite oil production plot for rich gas injection

Figure 4.12 shows that we have a single curve representing all PV injection runs. The individual curve for different PV injections branch out after breakthrough.

Similar plots for all the gases are shown in Appendix C.

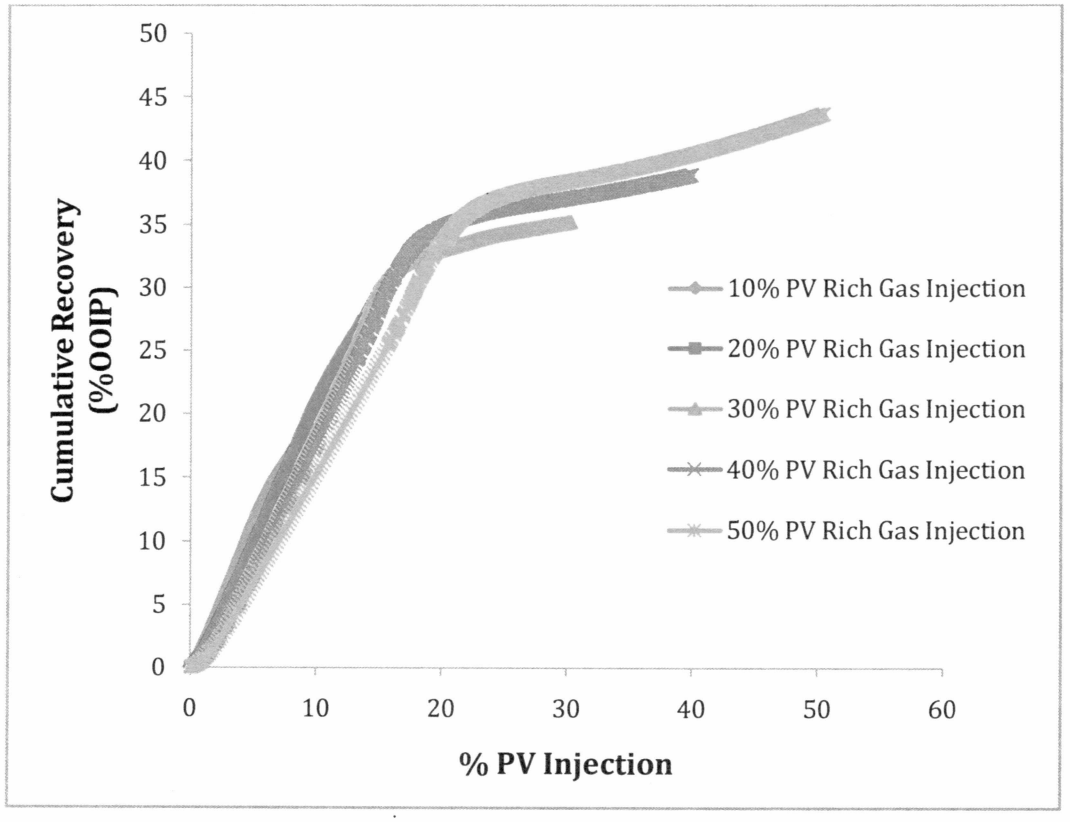

Figure 4.12: Recovery plot for rich gas injection

The change in the oil saturations in the reservoir over the period of time can also be monitored (Figure 4.13 to Figure 4.15). However, it is not practical to observe the phenomenon of viscous fingering in these profiles. This is because the size of the grid block is much larger than the length of the viscous finger. Viscous fingering usually takes place when a lighter phase displaces a much heavier phase. To observe viscous fingering, we will have to select a much finer grid size. (UAF has license for just 10000 grid blocks and the grid block sizing for the study was selected keeping this limitation in mind)

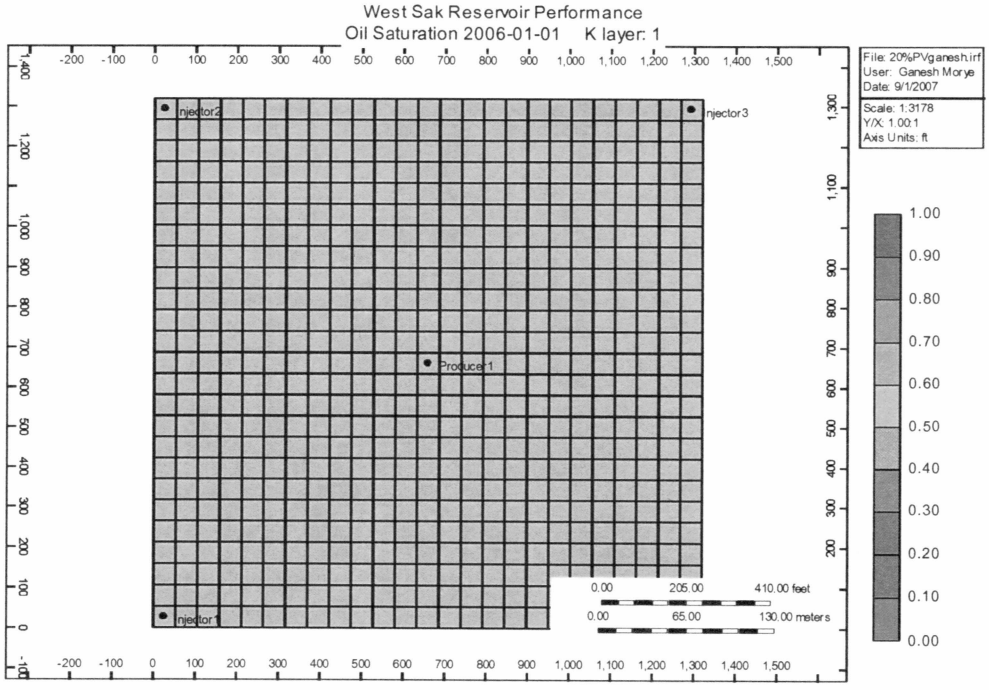

Figure 4.13: Oil saturation profile at time t=0 years

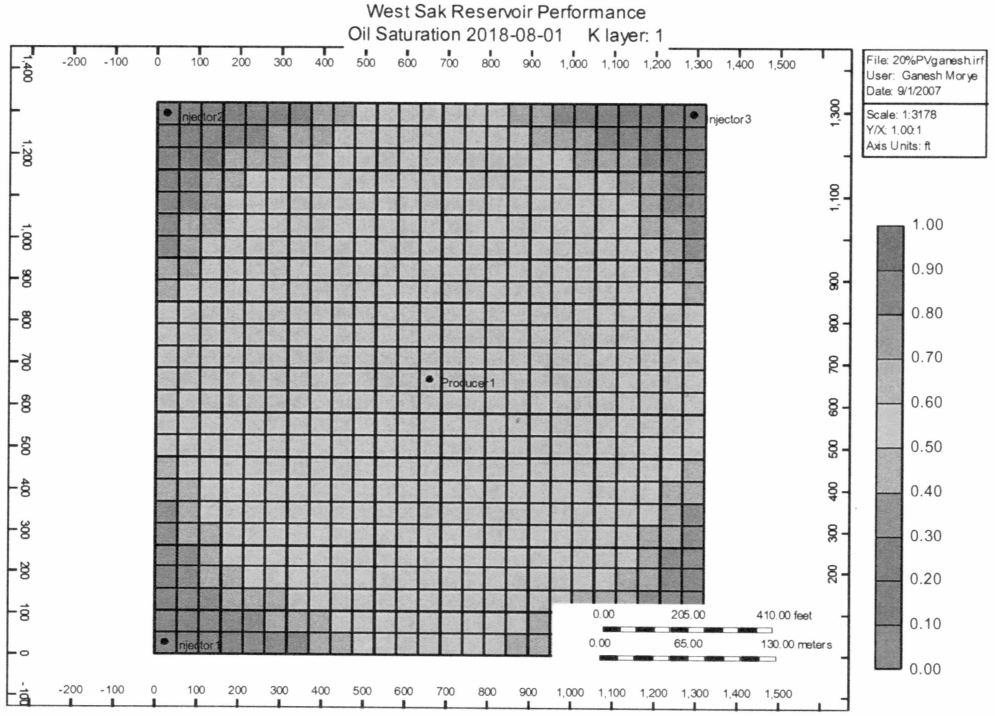

Figure 4.14: Oil saturation profile at time t=12 years

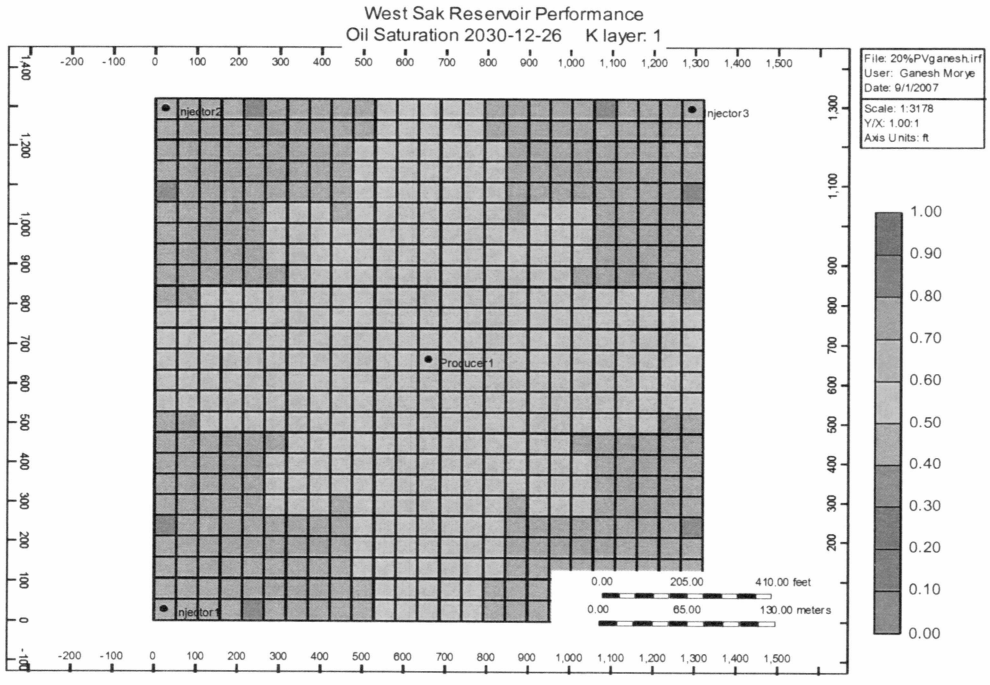

Figure 4.15: Oil saturation profile at time t=25 years

For CO_2 as an injection gas, it can be seen that a much earlier breakthrough is obtained (Figure 4.16 & Figure 4.17) as compared to the rich gas injection case. For a 10 % PV injection run, we don't see a clear breakthrough point. For a 20% PV injection run, breakthrough occurs around 12 years. With the increase in PV injection run we can see that breakthrough is achieved around 7.5 years for a 50% PV injection run. The cumulative recovery for a 20% PV injection run at breakthrough is 14.8% while the ultimate recovery for the entire project life is 18.75% (Figure 4.17). Thus we see that there is a slight increase in recovery even after breakthrough is achieved.

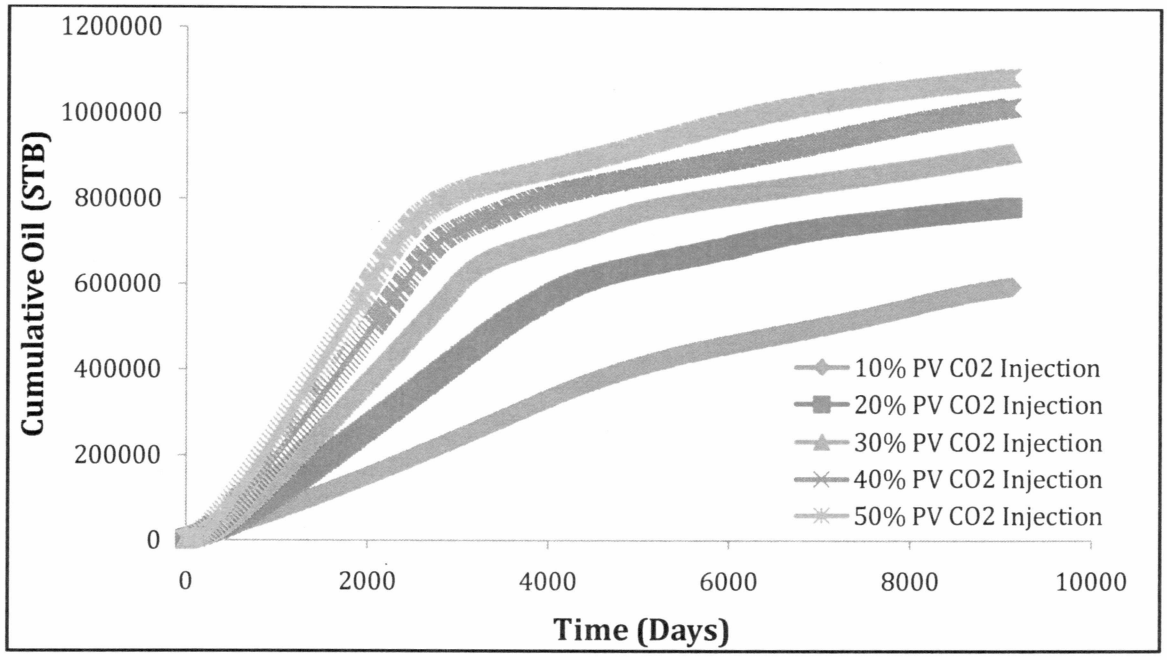

Figure 4.16: Composite cumulative oil production plot for CO_2 injection

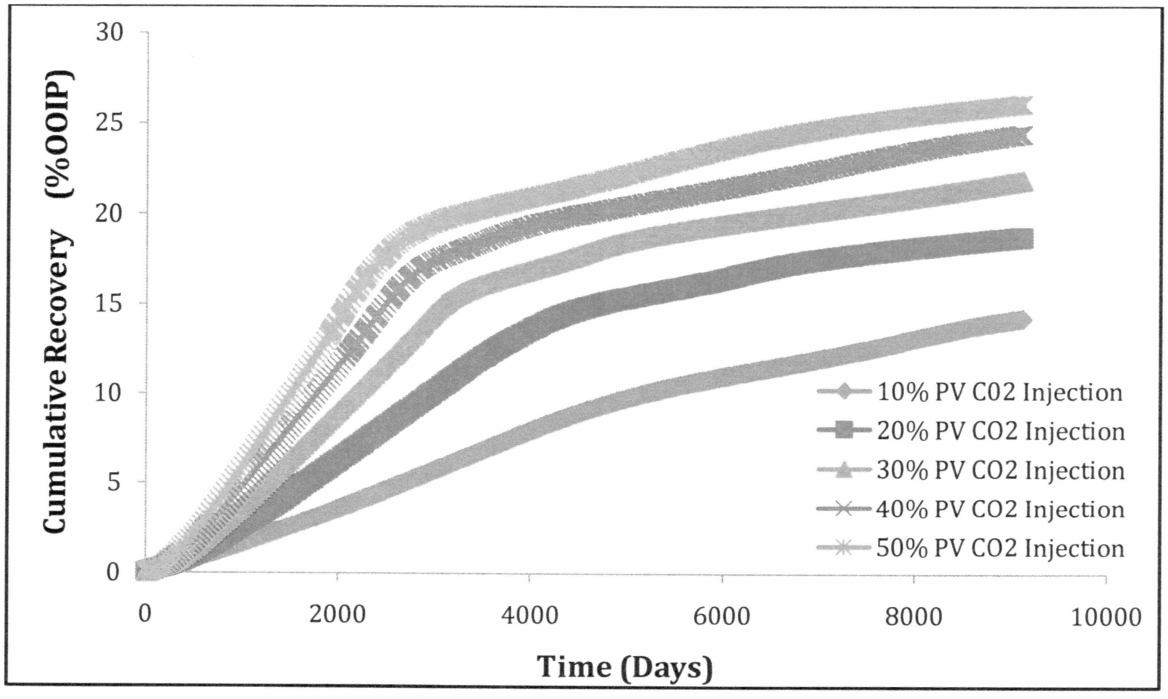

Figure 4.17: Composite cumulative oil recovery plot for CO_2 injection

For lean gas injection, we experience very early breakthrough (Figure 4.18 & Figure 4.19). Thus for a 10% PV injection run breakthrough is achieved in less than 7 years. The cumulative recoveries are far less as compared to the rich gas injection case. For a 50% PV injection run, ultimate recovery is just 14.9%. Also, not much oil is recovered after breakthrough.

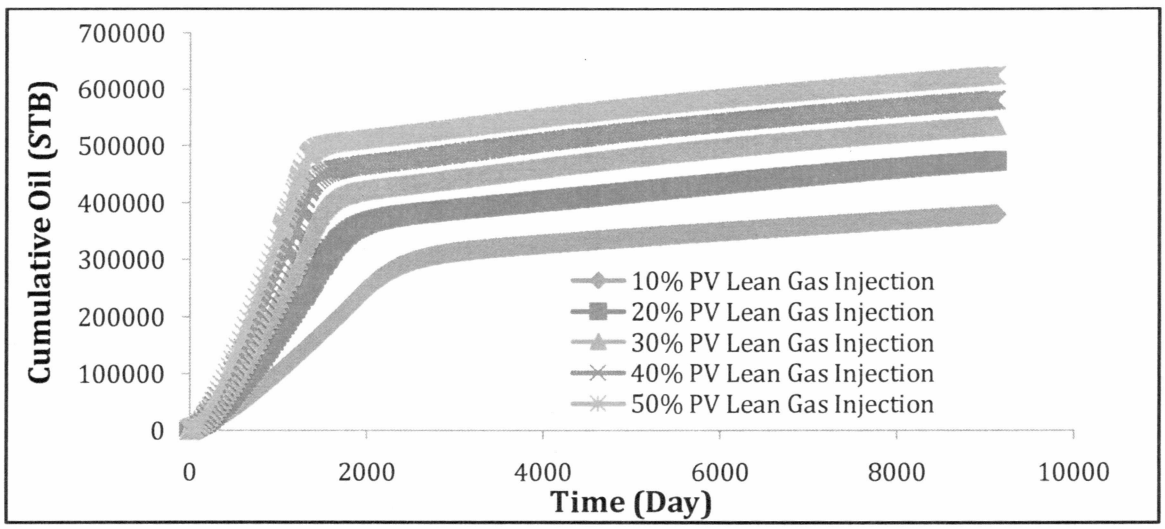

Figure 4.18: Composite cumulative oil production plot for lean gas injection

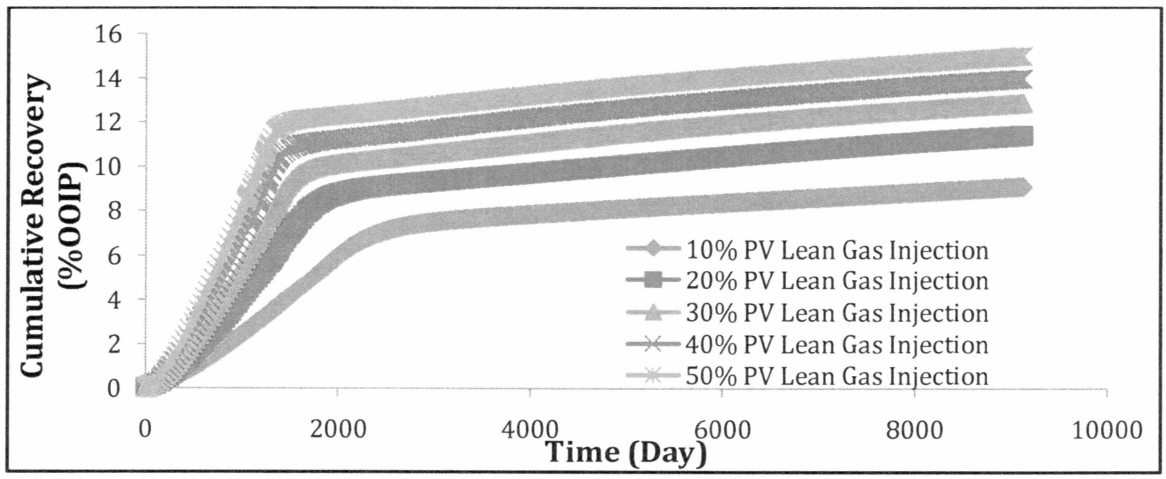

Figure 4.19: Composite cumulative oil recovery plot for lean gas injection

For PBG injection case (Figure 4.20 & Figure 4.21), we see a substantial amount of oil is recovered even after breakthrough is achieved. Thus for a 50% PV injection run, we see that the cumulative oil recovery at breakthrough is 17.5% while the ultimate recovery is 25.5%, indicating that a substantial amount of oil is recovered even after breakthrough.

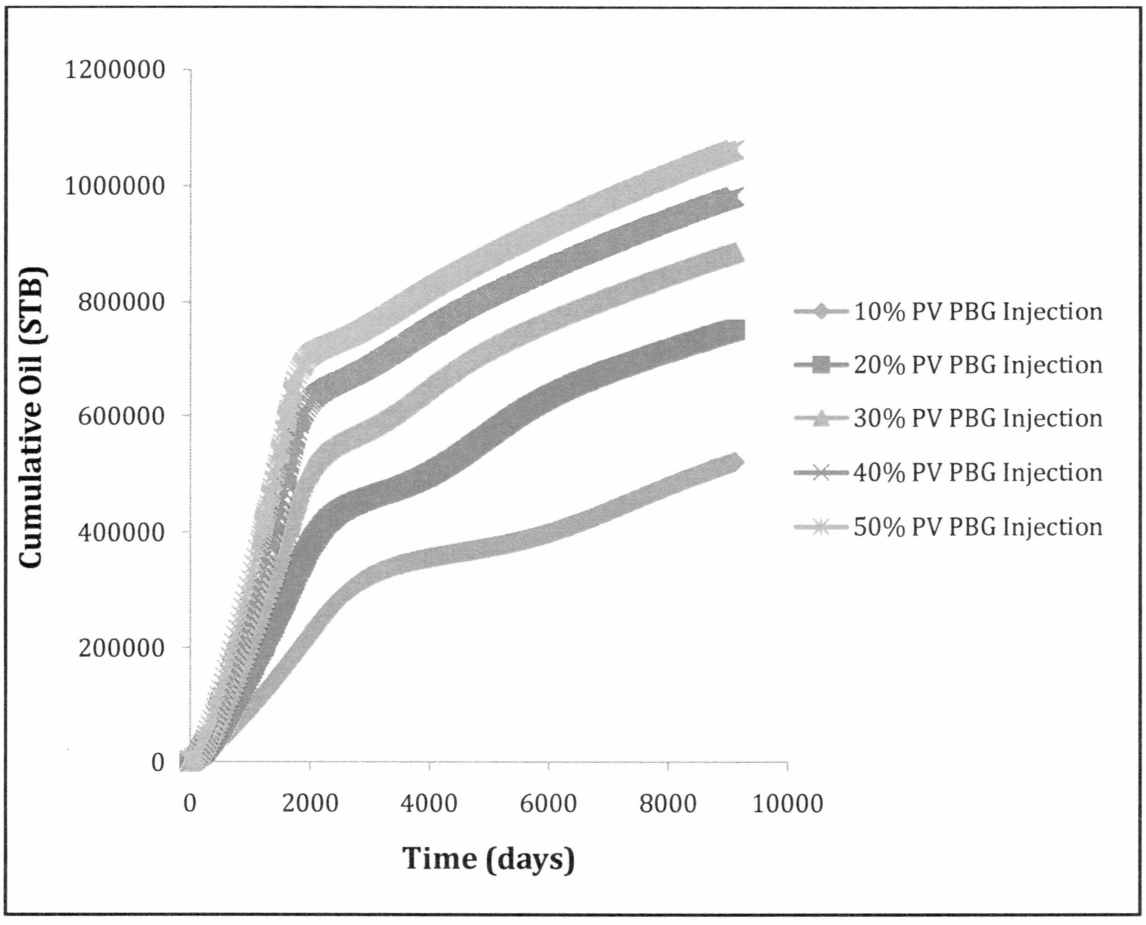

Figure 4.20: Composite cumulative oil production plot for PBG injection

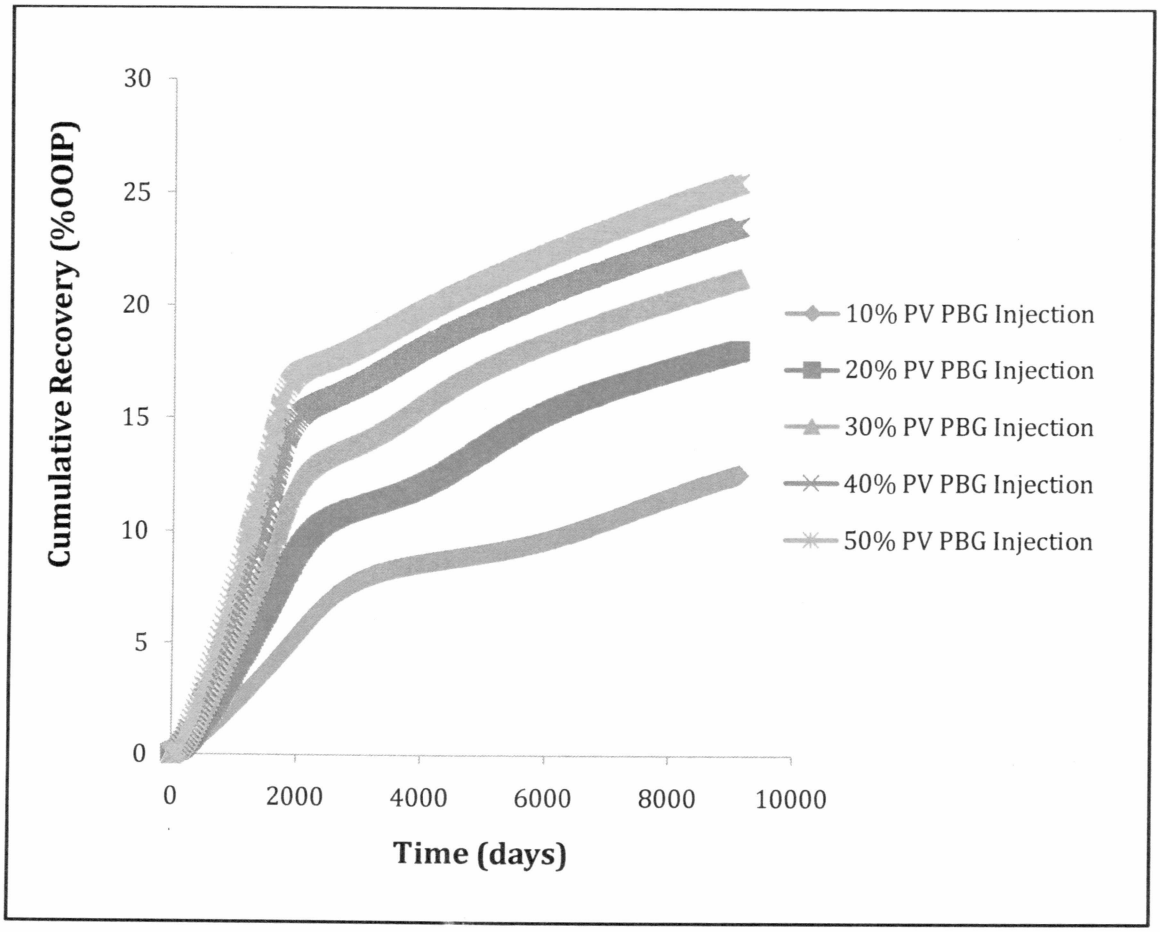

Figure 4.21: Composite cumulative oil recovery plot for PBG injection

In the case of West Sak VRI injection case too (Figure 4.22 & Figure 4.23), a substantial amount of oil is recovered even after breakthrough is achieved. Thus for a 50% PV injection run, the cumulative oil recovery at breakthrough is 17.5% and the ultimate oil recovery is 28.3%. Even though the recoveries at breakthrough for PBG and West Sak VRI are same, in case of West Sak VRI slightly more oil is recovered as compared to PBG injection case.

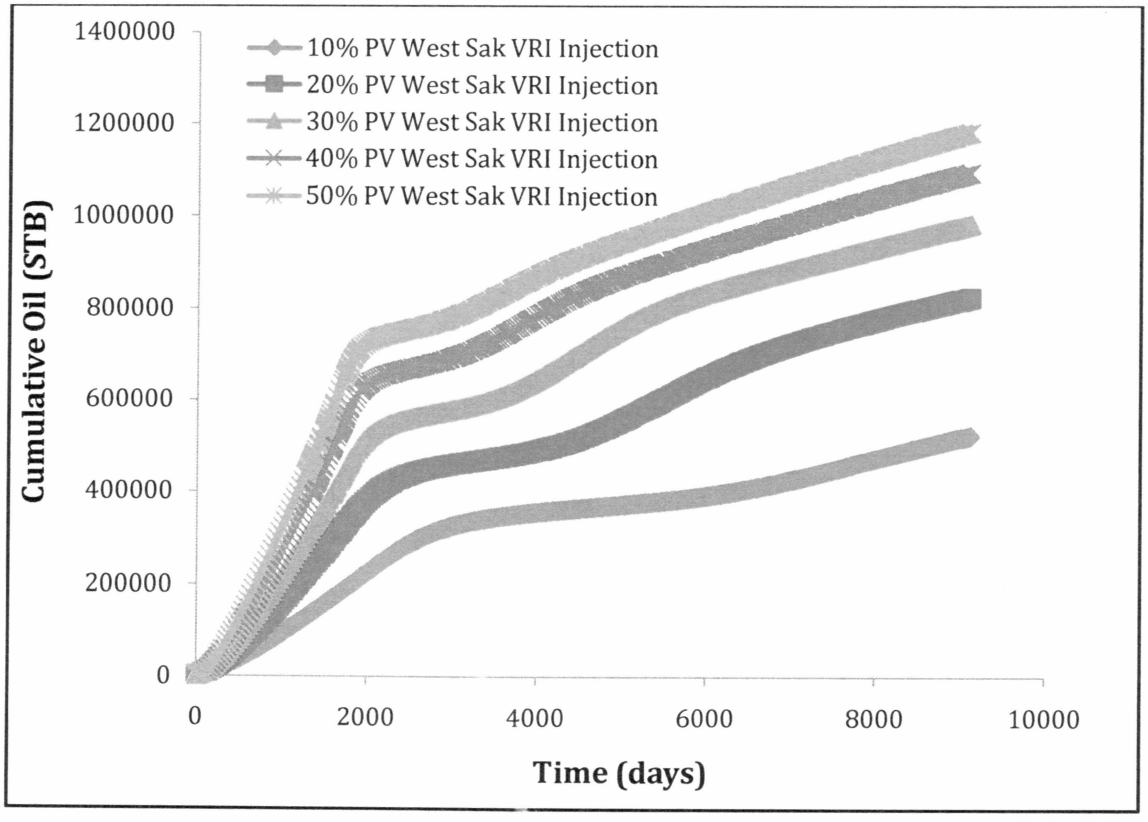

Figure 4.22: Composite cumulative oil production plot for West Sak VRI injection

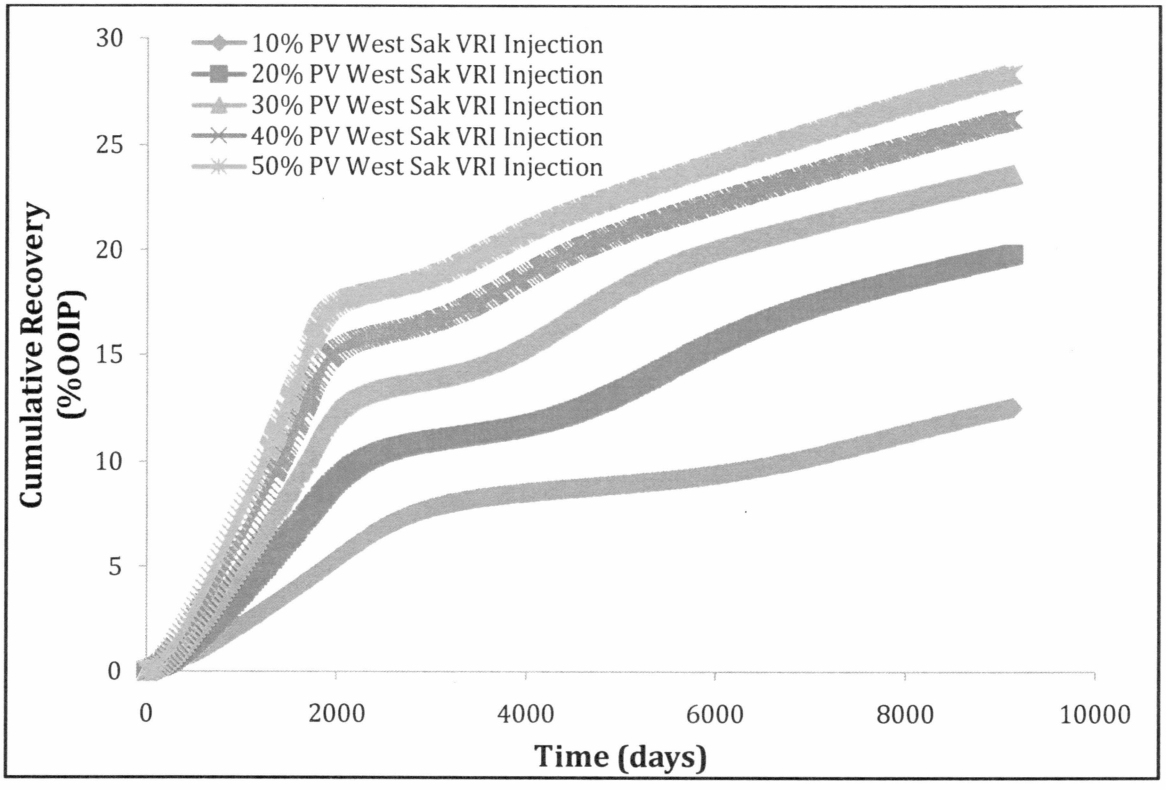

Figure 4.23: Composite cumulative oil recovery plot for West Sak VRI injection

Figure 4.24 is a composite plot of all the injection gases for a 30% PV injection case. As it can be seen, for the rich gas injection case, we experience a much delayed breakthrough as compared to other injection gases. Also the cumulative oil produced is much more for rich gas injection as compared to other gases. Figure 4.25 & Figure 4.26 are the recovery plots on dimensionless scale. It is seen that curves for different gases are represented by a single curve and it branches out after breakthrough for the respective gas is achieved. This kind of behavior is expected for any gas injection scheme and hence it verifies the authenticity of the simulation model.

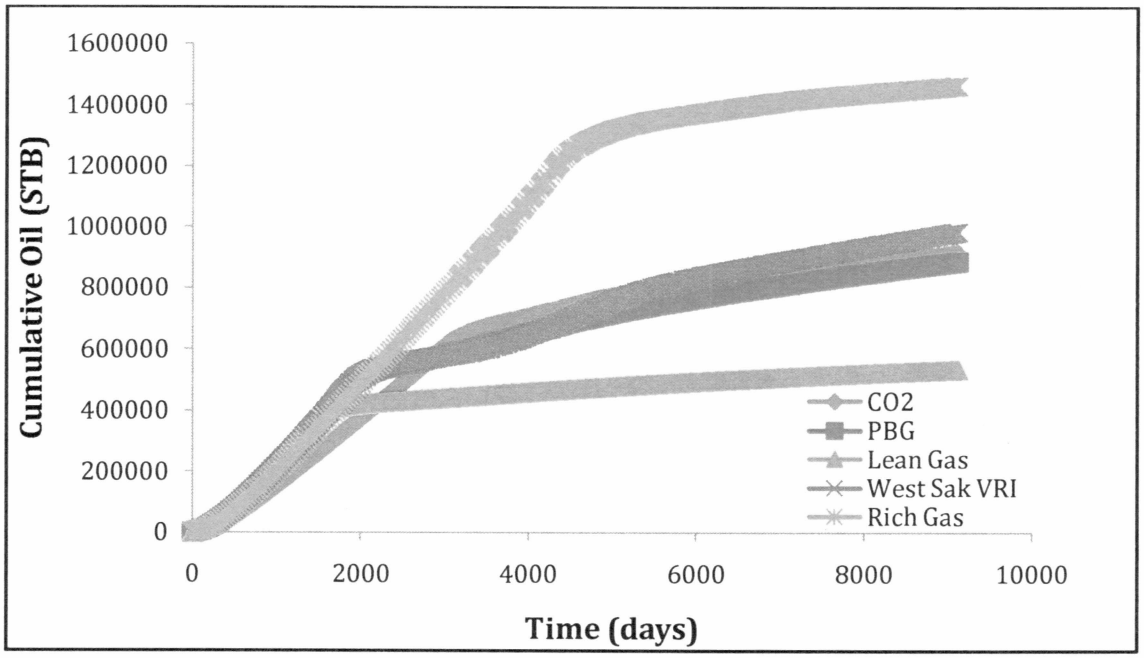

Figure 4.24: Composite cumulative oil produced plot for all the injection gases for 30% PV injection run

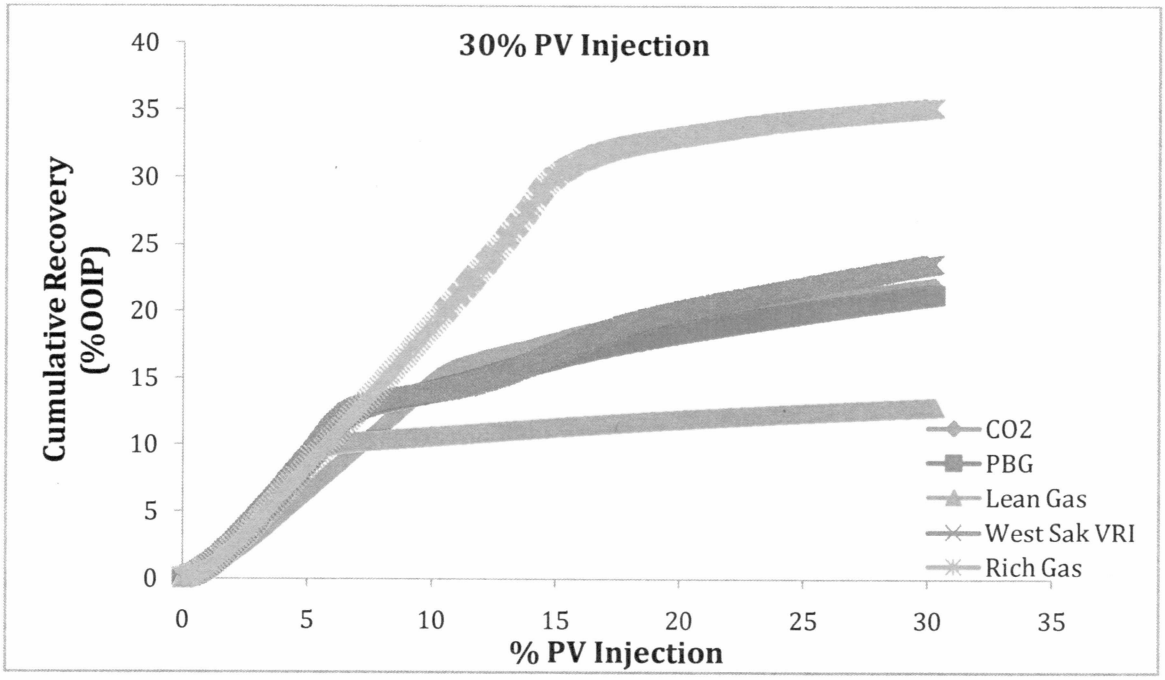

Figure 4.25: Composite cumulative recovery plot for all injection gases for 30% PV injection

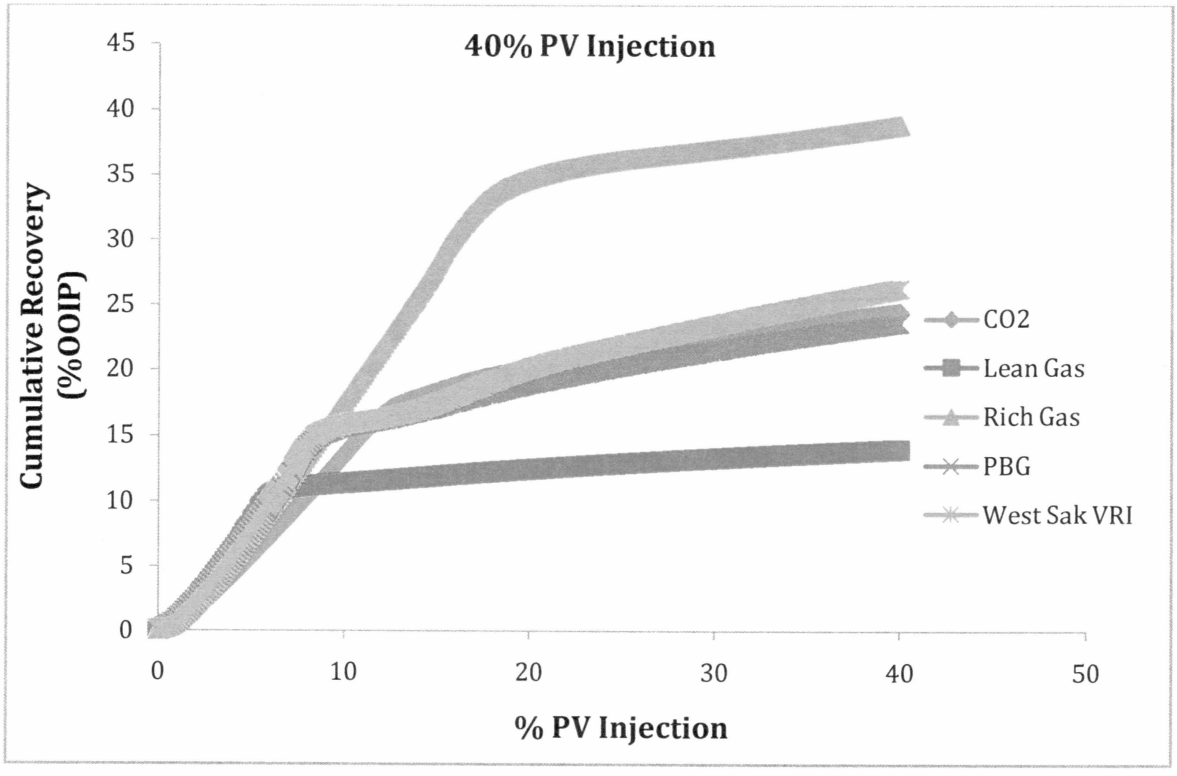

Figure 4.26: Composite cumulative recovery plot for all injection gases for 40% PV injection

Figure 4.27 gives direct comparisons for all the injection gases in terms of ultimate recoveries obtained. The ultimate recoveries of CO_2, West Sak VRI and PBG fall more or less in the same range. A much superior performance of rich gas injection is seen.

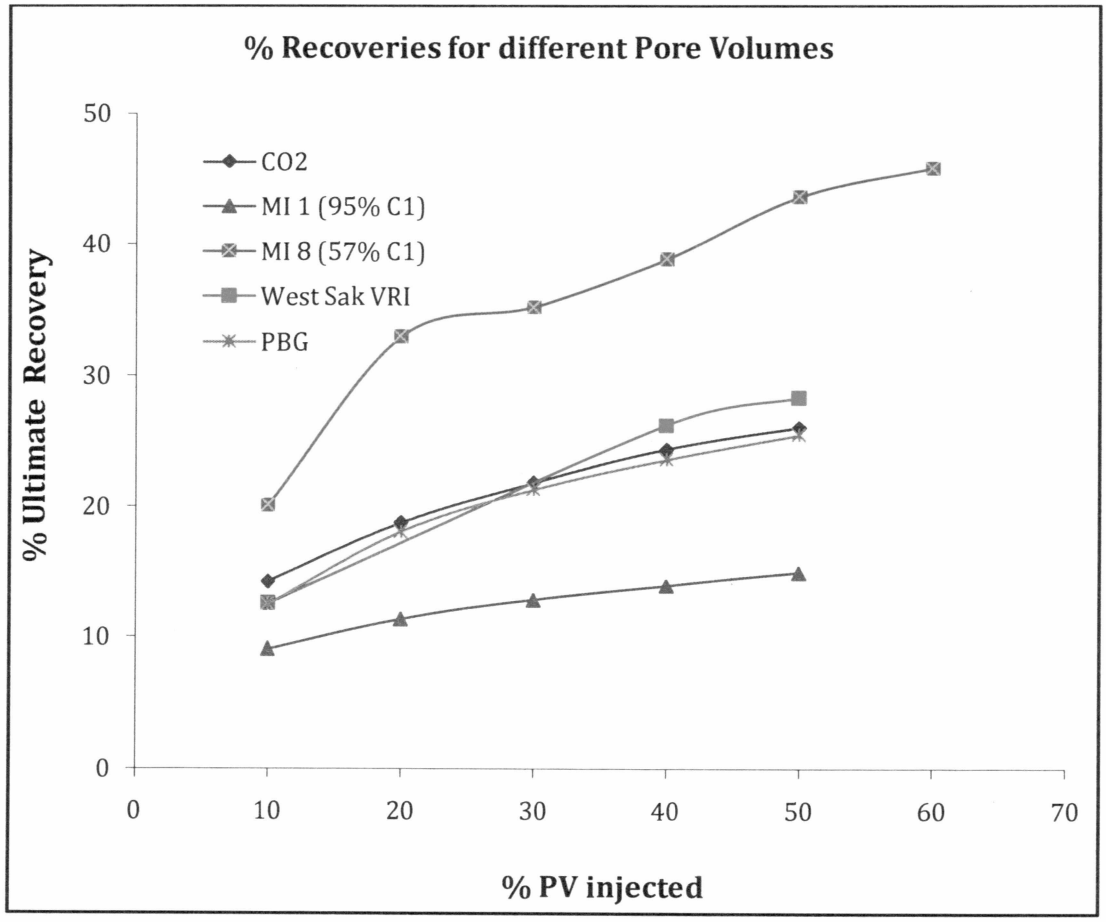

Figure 4.27: Comparison of ultimate recoveries obtained for all injection gases

4.2.2. Horizontal injection pattern

The performance of the reservoir under horizontal well injection was analyzed the same way as the vertical injection case. Accordingly, plots of cumulative production of oil and cumulative oil recovery versus time were studied (Figure 4.28 to Figure 4.31). Production profiles show similar trends. Cumulative recovery increases with the increase in PV of gas being injected. Recoveries obtained for respective PV are also plotted. Horizontal well is found to have little less recovery than the vertical well for a particular PV of gas being injected (Figure 4.32 & Figure 4.33). This is mainly because the horizontal well acts as a line drive because the producing layer is represented by only one grid block in the vertical or z-direction.

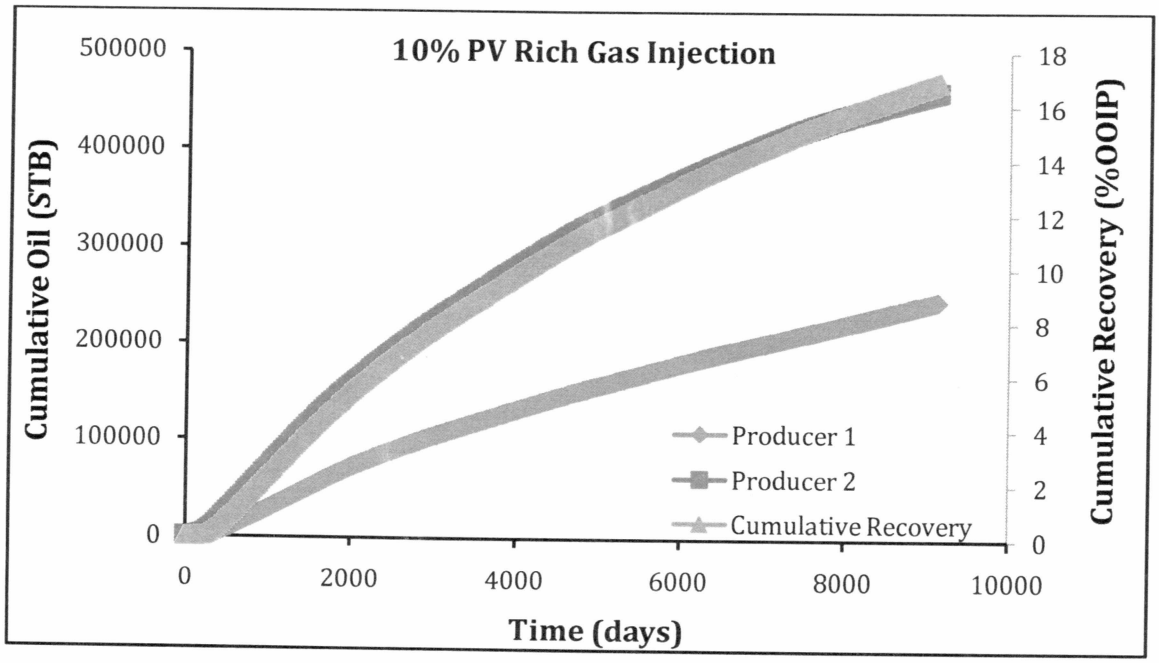

Figure 4.28: Cumulative oil produced and cumulative recovery obtained for 10% PV rich gas injection

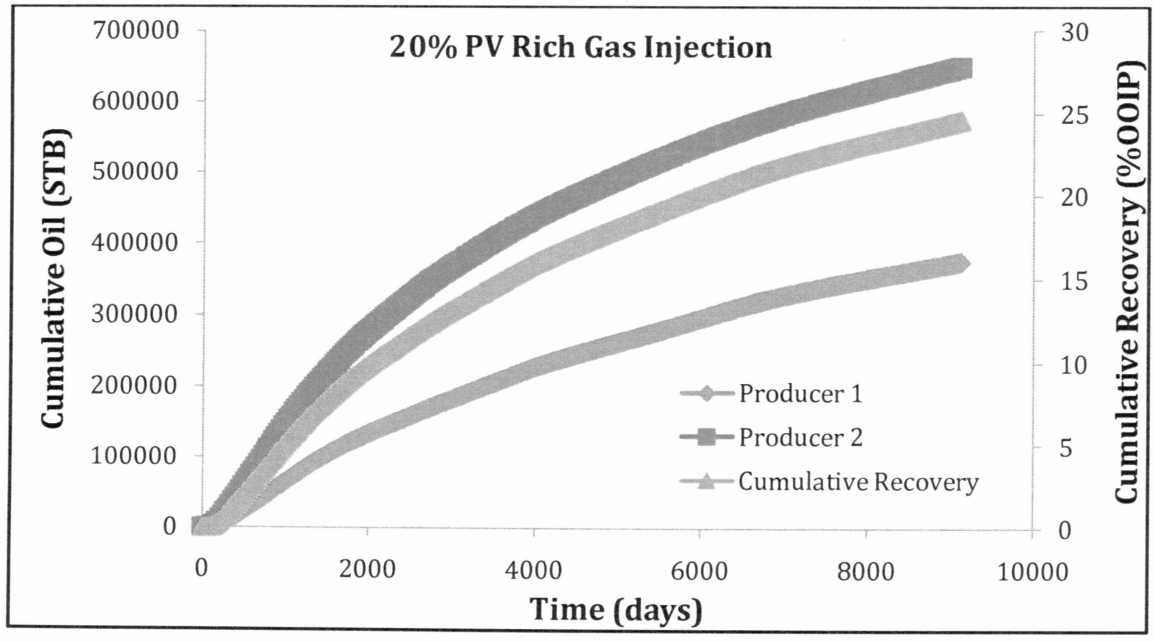

Figure 4.29: Cumulative oil produced and cumulative recovery obtained for 20% PV rich gas injection

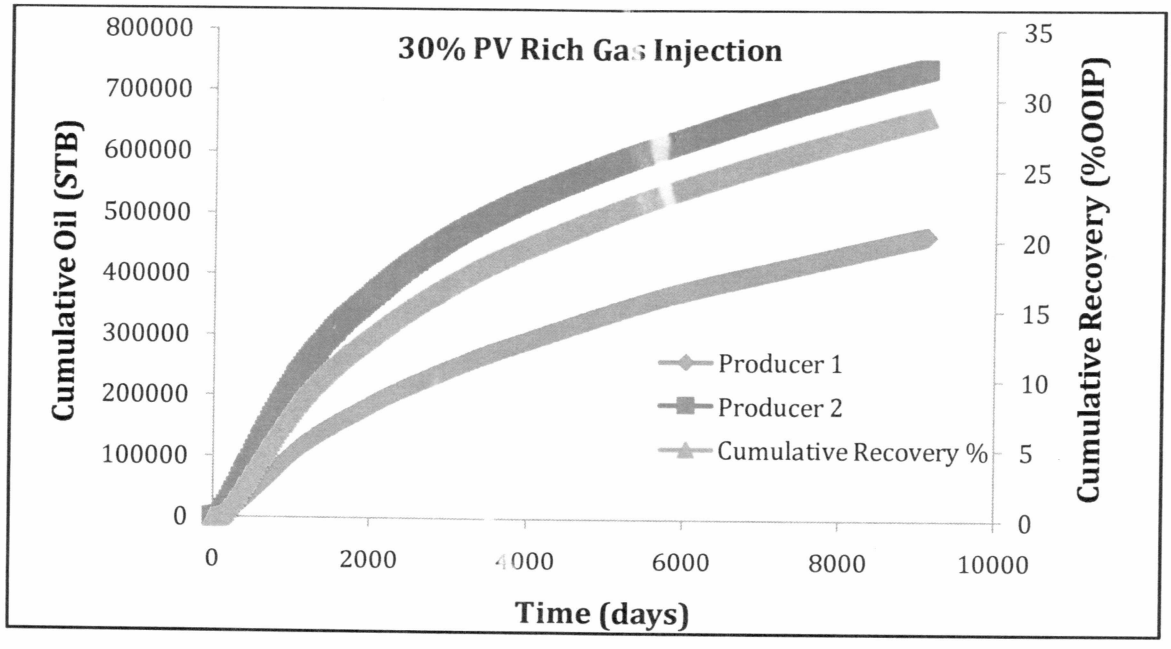

Figure 4.30: Cumulative oil produced and cumulative recovery obtained for 30% PV rich gas injection

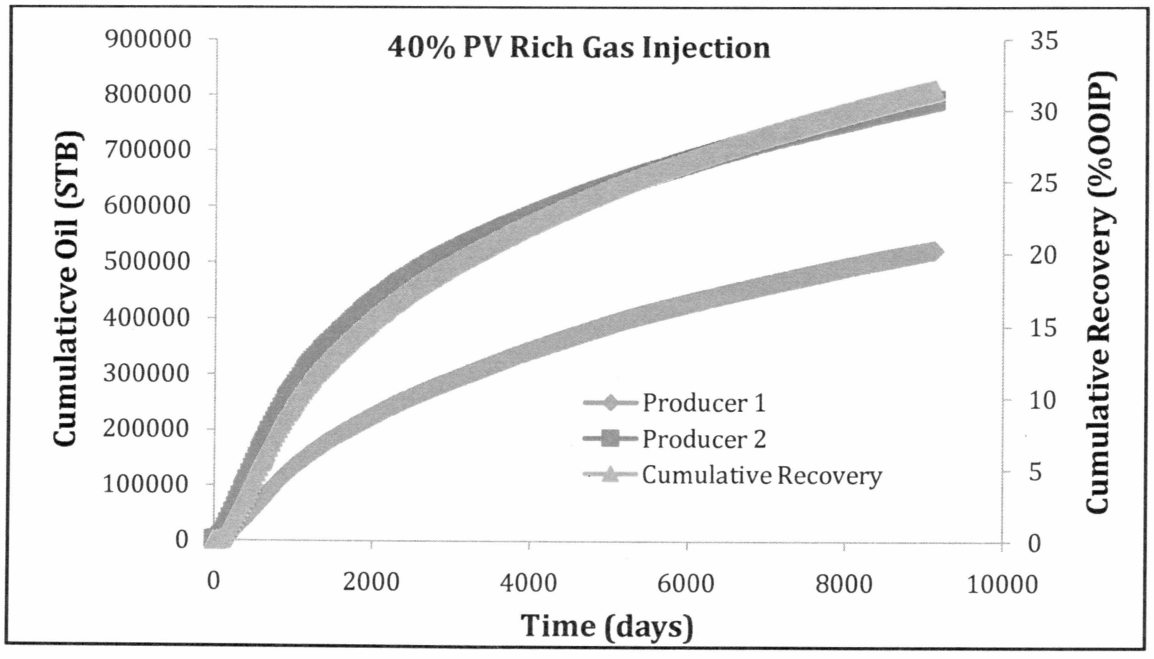

Figure 4.31: Cumulative oil produced and cumulative recovery obtained for 40% PV rich gas injection

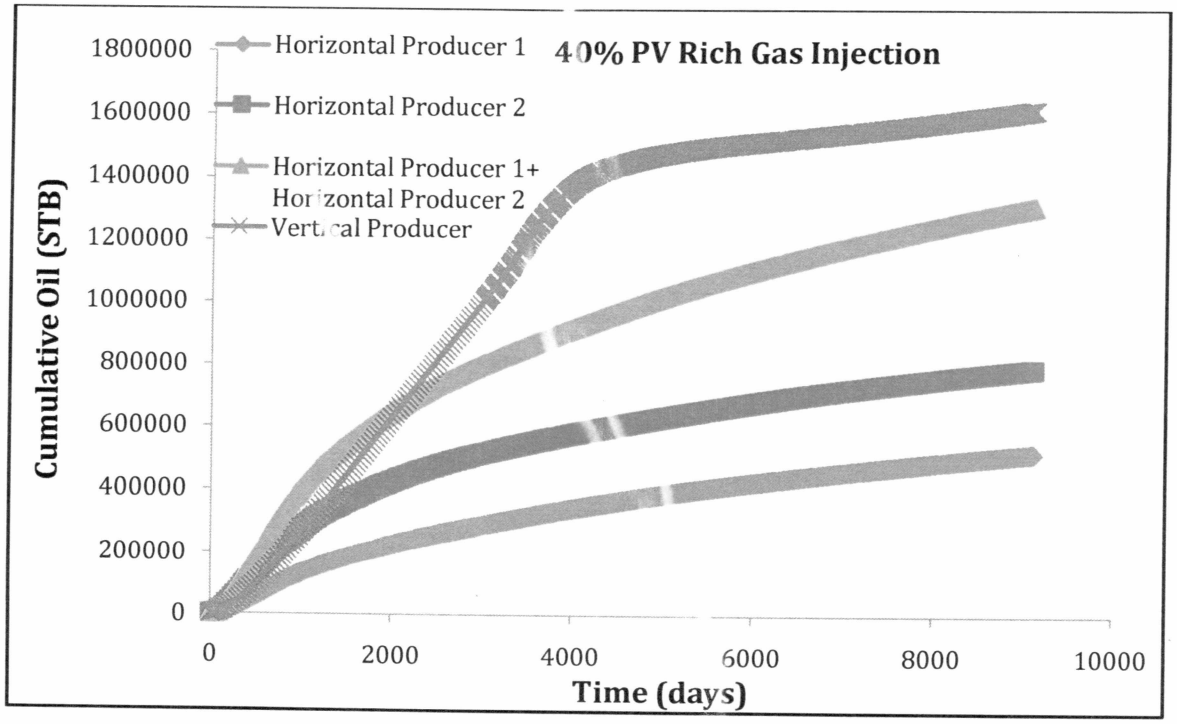

Figure 4.32: Comparison of performance between horizontal and vertical injection for a 40% PV rich gas injection

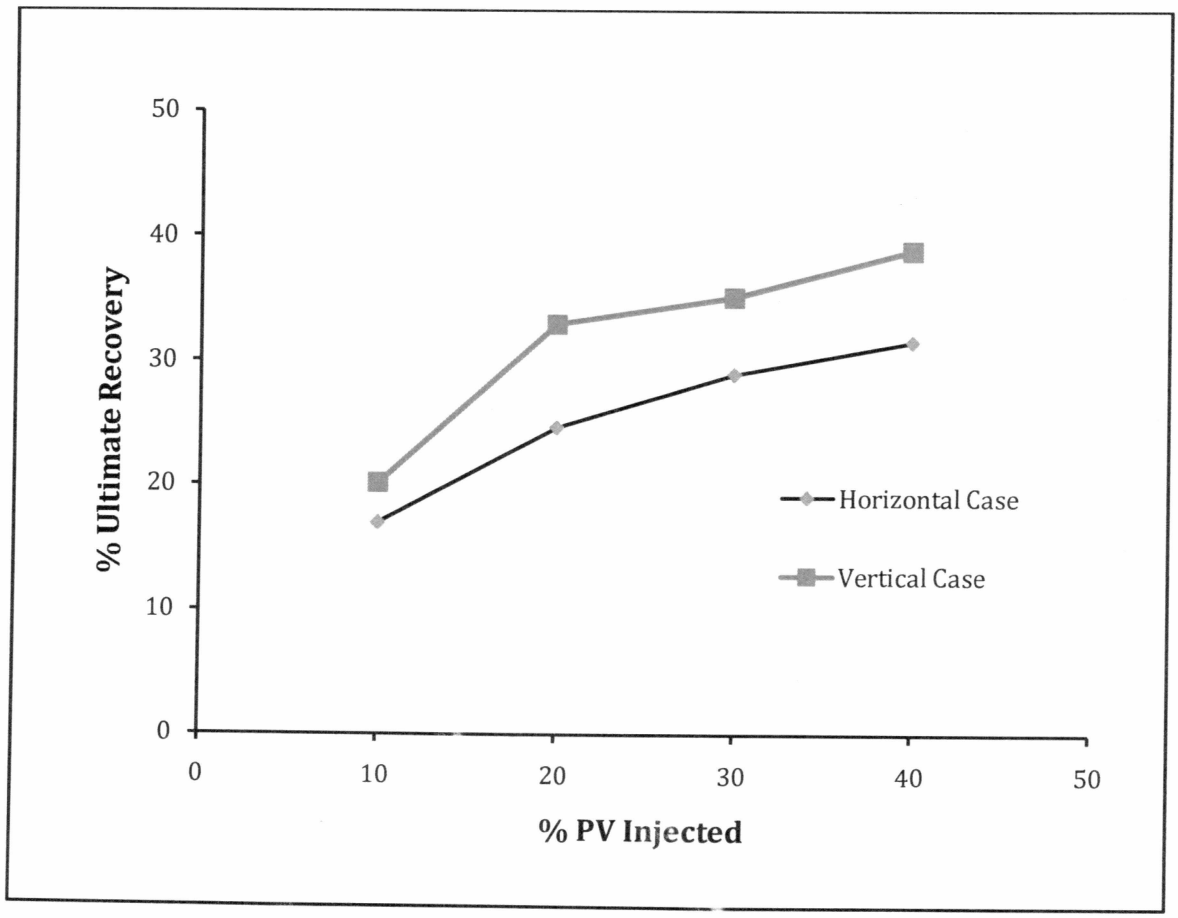

Figure 4.33: Comparison of ultimate recoveries for horizontal and vertical injection for rich gas injection

Chapter 5

Conclusions and Recommendations

5.1. Conclusions

- A thorough analysis of the capabilities of Peng-Robinson equation of state to predict the phase behavior of West Sak oil was carried out.
- It was found out that, in the absence of tuning; the EOS had inherent limitations which made its predictions flawed and unreliable.
- Better forecasts using the Peng Robinson EOS were obtained by tuning it to the experimental data.
- The validity of the tuned EOS was substantiated by the strong agreement of the tuned EOS predicted values with the experimental values.
- Enhanced oil recovery using gas injection for production of the viscous West Sak oil was explored using reservoir simulation software CMG GEM. It was found out that substantial increase in oil recoveries can be accomplished with proper selection of injectant gas and reservoir operating conditions.
- The enhancements in recoveries that can be achieved vary from gas to gas. It depends upon flow conditions that are attainable for a particular gas. Miscibility between the injected gas phase and the oil produced plays a pivotal role in determining this.
- It was found that recoveries for a rich gas were as high as 44% for a 50% PV injection indicating it might be achieving miscible flow. The recoveries for an immiscible lean gas were extremely low strongly supporting the advantage of a single phase miscible flow.

- The reservoir model built had limitations in the form of the number grid blocks that can be selected. Due to this, the vertical 5-spot injection pattern yielded slightly better recoveries as compared to the horizontal injection scheme used in the study. The main reason for this was that the horizontal well was essentially acting as a line drive and a 5-spot pattern always performs better than a line drive.

5.2. Recommendations

Although experimental data in the form of differential liberation, constant composition expansion was available and it greatly aided the tuning process, for a thorough phase behavior study additional experimental data such as separator test and more importantly, data for static and equilibrium tests such as slim-tube, is of prime importance to successfully incorporate phase changes in the presence of additional solvents in the EOS.

Even though gas injection seems to be a lucrative option for increasing oil recovery, the main factor which will drive its selection as an EOR technique will be the economics involved. Since miscibility is the main driving force for the improvement in recovery, it will require proper designing of the injectant gas. Such a designing scheme will require thorough investigation of things, such as availability of the parent gas which will be enriched, facilities like the mixing equipment, storage etc. The economics will have to be extensively worked upon, even though the process looks technically profitable.

References

Al-Meshari, A.A., Aramco, S., McCain, W.D. (2005). New Strategic Method to Tune Equation-of-State for Compositional Simulation. *Presented at the Technical Symposium of Saudi Arabia Section, SPE 106332.* Dahrahn, Saudi Arabia.

Anna, D. (2005). *DOE-Fossil Energy Techline-Heavy Oil Potential Key to Alaska North Slope Oil Future.* Retrieved August 16, 2007, from Fossil Energy Techline: http://www.fossil.energy.gov/news/techlines/2005/tl_alaska_oil.html

Bakshi, A.K. (1991). Computer Modeling of CO_2 Stimulation in the West Sak Reservoir. *M.S. Thesis, University of Alaska Fairbanks* . Fairbanks.

Bakshi, A.K., Ogbe, D.O., Kamath, V.A, Hatzignatiou, D.G. (1992). Feasibilty Study of CO_2 Stimulation in the West Sak Field, Alaska. *Presented at the Western Regional Meeting, SPE 24038.* Bakersfield, California.

Coats, K.H. (1982). Reservoir Simulation: State of the Art. *Journal of Petroleum technology* , Vol. 34, No. 8, pp.1633-1642.

Coats, K.H. & Smart, G.T. (1986). Application of a Regression-Based EOS PVT Program to Laboratory Data. *SPE Reservoir Engineering* , Vol. 1, No. 3, pp. 277-299.

DeRuiter, R.A., Nash, L.J., Singletary, M.S. (1994). Solubility and Displacement Behavior of a Viscous Crude With $CO_2$and Hydrocarbon Gases. *SPE Reservoir Engineering* , Vol. 9, No. 2, pp. 101-106.

Green, D.W. & Willhite, G.P. (1998). *Enhanced Oil Recovery.* Richardson, Texas: Society of Petroleum Engineers.

Holt, T. (2003). *http://www.force.org/fresco/seminar2003/Abstracts/simulation_Sintef.htm.* Retrieved from http://www.force.org/: http://www.force.org/fresco/seminar2003/Abstracts/simulation_Sintef.htm

Joergensen, M. & Stenby, E.H. (1995). Optimization of Pseudo-component Selection for Compositional Studies of Reservoir Fluids. *Presented at the 70th Annual Technical COnference and Exhibiton, SPE 30789.* Dallas, Texas.

Katz, D.L., (1983). Overview of Phase Behavior of Oil and Gas Production. *Journal of Petroleum Technology*, Vol. 35, No. 6, pp. 1205-1214.

Kesler, G. & Lee, I. (1976). Improve Prediction of Enthalpy of Fractions. *Hydrocarbon Processing*, Vol. 55, pp. 153-158.

Lawrence, J., Teletzke, G., Hutfilz, J., Wilkinson, J. (2003). Reservoir Simulation of Gas Injection Process. *Presented at the 13th Middle East Oil Show & Conference, SPE 81459.* Bahrain.

Lee, S., Moulds, T.P., Narayan, R., Youngren, G., Lin, C., Wang, Y. (2001). Optimizing Miscible Injectant (MI) Compositions for Gas Injection Projects. *Presented at the SPE Annual Technical Conference, SPE 71606.* New Orleans, Louisiana.

Liu, K. (1999). Fully Automatic Procedure for Efficient Reservoir Fluid Characterization. *Presented at the SPE Annual Technical Conference and Exhibition, SPE 56744.* Houston, Texas.

McGuire, P.L., Redman, R.S., Jhaveri, B.S., Yancey, K.E., Ning, S.X. (2005). Viscosity Reduction WAG: AN Effective EOR Process for North Slope Viscous Oils. *Presented at the SPE Western Regional Meeting, SPE 93914.* Irvine, California.

Patil, S.B. (2006). Investigation of CO_2 Sequestration Options for Alaska North Slope With Emphasis on Enhanced Oil Recovery. *M.S. Thesis, University of Alaska Fairbanks*. Fairbanks.

Patil, S.L. & Dandekar, A.Y. (2004). *Phase Behavior, Solid Organic Precipitation and Mobility Characterization Studies in Support of Enhanced Heavy Oil Recovery on Alaska North Slope. Research Proposal* Fairbanks, AK: University of Alaska Fairbanks.

Riazi, M.R. & Daubert, T.E. (1980). Simplify Property Predictions. *Hydrocarbon Processing*, 115-116.

Sharma, A.K. (1988). A Slim-Tube Study of Solvents For The Miscible Displacement of West Sak Crude. *M.S. Thesis, University of Alaska Fairbanks*. Fairbanks.

Sharma, A.K., Patil, S.L., Kamath, V.A., Sharma, G.D. (1989). Miscible Displacement of Heavy West Sak Crude by SOlvents in Slim Tube. *Presented at the California Regional Meeting, SPE 18761.* Bakersfield, California.

Sharma, G.D. (1990). *Development of Effective Gas Solvents Including Carbon Dioxide For The Improved Recovery of West Sak Oil.* Fairbanks: University of Alaska Fairbanks.

Sharma, G.D. (1993). *Charaterization of Oil and Gas Heterogeneity.* Fairbanks: University of Alaska Fairbanks.

Sharma, G.D., Kamath, V.A, Godbole, S.P., Patil, S.L. (1988). The Potential of Natural Gas in the Alaskan Arctic. *Presented at the California Regional Meeting, SPE 17456.* Long Beach, California.

Speight, J. G. (1991). The Chemistry and Technology of Petroleum. New YorK: Marcel Dekker, Inc.

Targac, G.W., Redman, R.S., Davis, E.R., Rennie, S.B., McKeveer, S. (2005). Unlocking the Value of West Sak Heavy Oil. *Presented at the SPE International Thermal Operation and Heavy Oil Symposium, SPE 97856.* Calgary, Canada.

Twu, H. (1984). An Internally Consistent for Predicting the Critical Properties and Molecular Weights of Petroleum and Coal-Tar Fluids. *Fluid Phase Equilibria* , Vol. 16, 137-150.

Twu, C., Tilton, B., Bluck, D. (2007.). *The Strengths and Limitations of Equation of State Models and Mixing Rules.* Retrieved August 2007, from SmiSci-Esscor, Simulation Software for Plant Design and Optimization: http://www.simsci-esscor.com/NR/rdonlyres/3A5E699D-3EEB-4B43-A04C-3F1922585FFA/0/31099.pdf

Wang, P. & Pope, G. (2001). Proper Use of Equations of State for Compositional Reservoir Simulation. *Journal of Petroleum Technology* , Vol. 53, No. 7, pp. 74-81.

Whitson, C.H. (1983). Characterizing Hydrocarbon Plus Fraction. *SPE* , Vol. 23, No. 4, pp. 683-694.

Glossary

Symbols

m = Dimensionless parameter
n = Exponent
P = Pressure, psia
R = Gas constant, 10.73 psi-ft^3/lb-mol ^oR
T = Temperature, ^oR
Z = Compressibility factor
z = Mole fraction
α = Dimensionless parameter
ω = Acentric factor

Abbreviations

ANS = Alaska North Slope
BIN = Binary Interaction Parameters
BPXA = British Petroleum Exploration (Alaska), Inc
CCE = Constant Composition Expansion
CMG = Computer Modeling Group
DL = Differential Liberation
EOS = Equation of State
GEM = Generalized Equation of State Model
MCN = Multi-Carbon Number
MI = Miscible Injectant
MW = Molecular Weight
PBG = Prudhoe Bay Gas
PR = Peng Robinson
PVT = Pressure-Volume-Temperature
SCN = Single Carbon Number
SG = Specific Weight
VRI = Viscosity Reducing Injectant

Subscripts

c = critical
r = reduced

Appendix A

Table A-1: Compositional and physical property data for West Sak oil (Sharma, 1990)

Components	Composition	Pc atm	Tc K	Acentric Factor	Mol Wt
CO_2	0.016	72.8	304.2	0.225	44.01
N2	0.032	33.5	126.2	0.04	28.013
C1	38.333	45.4	190.6	0.008	16.043
C2	0.857	48.2	305.4	0.098	30.07
C3	0.359	41.9	369.8	0.152	44.097
NC4	0.179	37.5	425.2	0.193	58.124
NC5	0.064	33.3	469.6	0.251	72.151
FC6	0.2	32.46	507.5	0.275	86
FC7	0.016	30.97	543.2	0.3083	96
FC8	0.008	29.12	570.5	0.3513	107
FC9	0.823	26.94	598.5	0.3908	121
FC10	1.496	25.01	622.1	0.4438	134
FC11	1.72	23.17	643.6	0.4775	147
FC12	1.346	20.43	682.4	0.5596	175
FC13	1.496	21.63	663.9	0.5223	161
FC14	1.795	19.33	700.7	0.6048	190
FC15	1.944	18.25	718.6	0.6512	206
FC16	1.795	17.15	734.5	0.6837	222
FC17	1.57	16.35	749.2	0.7286	237
FC18	1.795	15.65	760.5	0.7574	251
FC19	2.468	15.06	771	0.7901	263
FC20	2.841	14.36	782.9	0.8161	275
C21+	39.037	9.976	960.84	1.1298	455

Table A-2: Differential liberation data (Sharma, 1990)

P psia	OIL FVF bbl/STB	GOR SCF/STB	z	Gas FVF	Gas SG	Oil viscosity cP
1704.7	1.07	207				45.2
1514.7	1.062	187	0.831	0.00834	0.571	50.2
1314.7	1.055	165	0.843	0.00976	0.579	51.8
1114.7	1.047	144	0.866	0.01182	0.567	59.3
914.7	1.04	124	0.887	0.01475	0.568	68.6
714.7	1.033	96	0.909	0.01936	0.568	83.4
514.7	1.026	70	0.933	0.02757	0.574	
314.7	1.019	42	0.951	0.04555		
114.7	1.012	11	0.985	0.1306	0.575	
14.7	1.008	0			0.661	272.7

Table A-3: Constant composition expansion data (Sharma, 1990)

P psia	ROV	Vol%
7014.7	0.972	
6514.7	0.974	
6014.7	0.977	
5514.7	0.98	
5014.7	0.983	
4514.7	0.986	
4014.7	0.989	
3514.7	0.991	
3014.7	0.994	
2514.7	0.996	
2064.7	0.998	
1764.7	0.9996	
1714.7	0.9999	
1704.7	1	1
1447.7	1.032	0.974
1372.7	1.045	0.954
1258.7	1.067	0.934
1120.7	1.102	0.894
1021.7	1.134	0.878
907.7	1.18	0.844
818.7	1.227	0.798
705.7	1.305	0.762
594.2	1.415	0.685
460.2	1.622	0.605

Table A- 4: Composition of the injectant gases

Components	**West Sak VRI** (McGuire, et al. 2005)	**MI 1** (Lee, 2001)	**MI 8** (Lee, 2001)	**PBG** (Sharma A. , September 1988)
C1	78.052	95.900	57.842	72.675
C2	8.929	3.900	7.393	7.863
C3	5.879	0.100	19.381	4.916
C4	4.240	0.000	15.285	1.469
C5	1.100	0.000	0.000	0.520
C6	0.210	0.000	0.000	0.240
C7+	0.040	0.100	0.100	0.140
CO_2	1.210	0.000	0.000	12.179
N_2	0.000	0.000	0.000	0.000

Appendix B

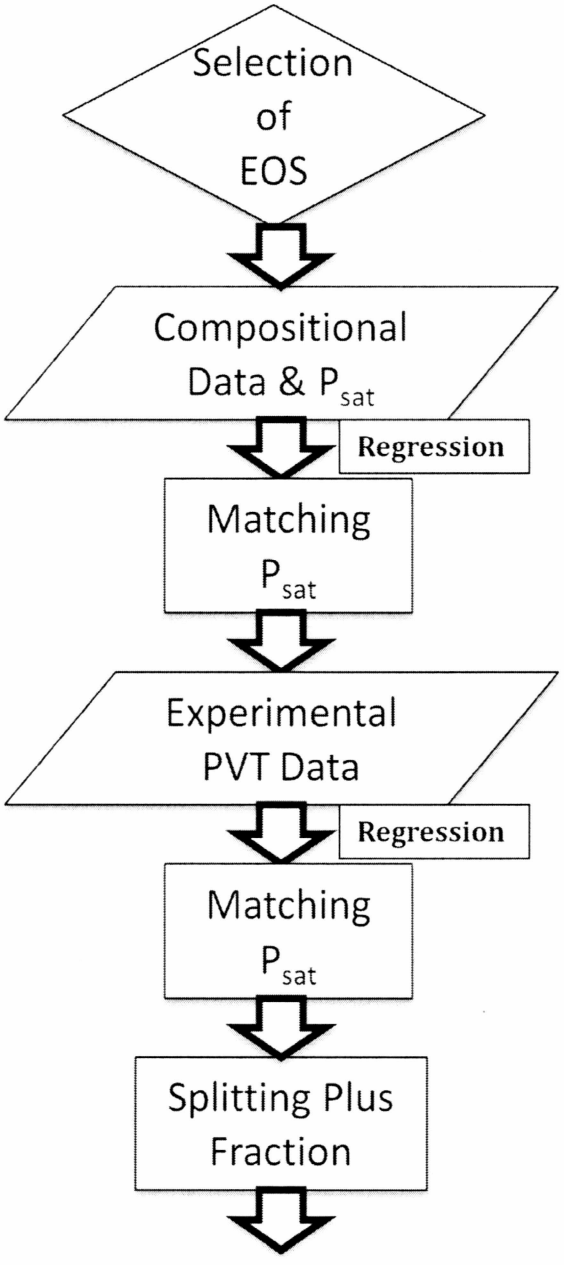
Selection of EOS
Compositional Data & P_{sat}
Regression
Matching P_{sat}
Experimental PVT Data
Regression
Matching P_{sat}
Splitting Plus Fraction

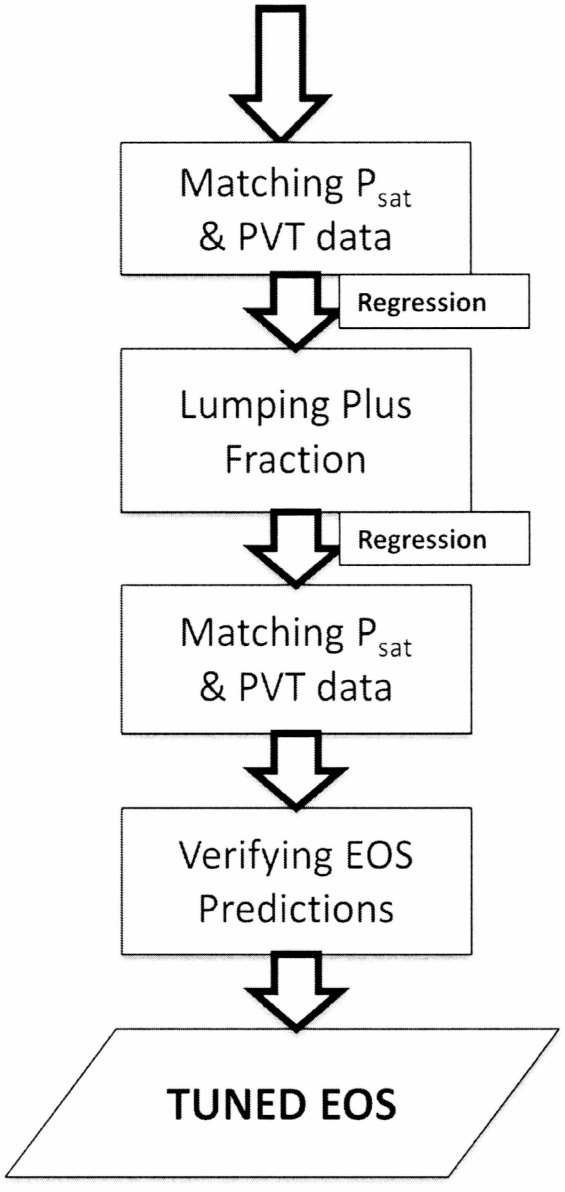

Figure B-1: Flow chart showing the steps involved in tuning

Appendix C

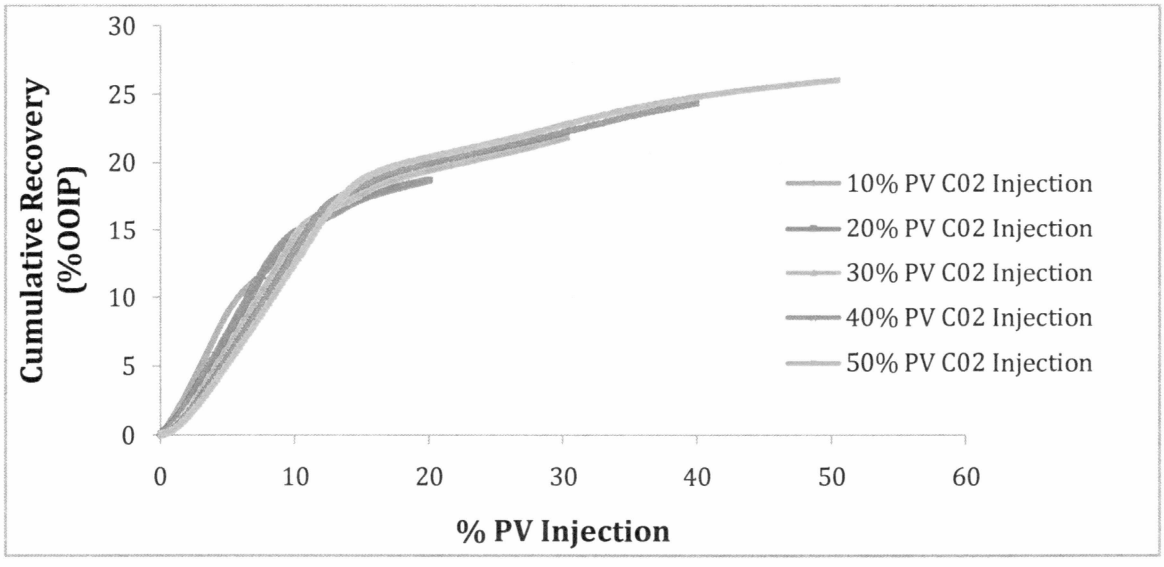

Figure C 1: Recovery plot for CO_2 injection

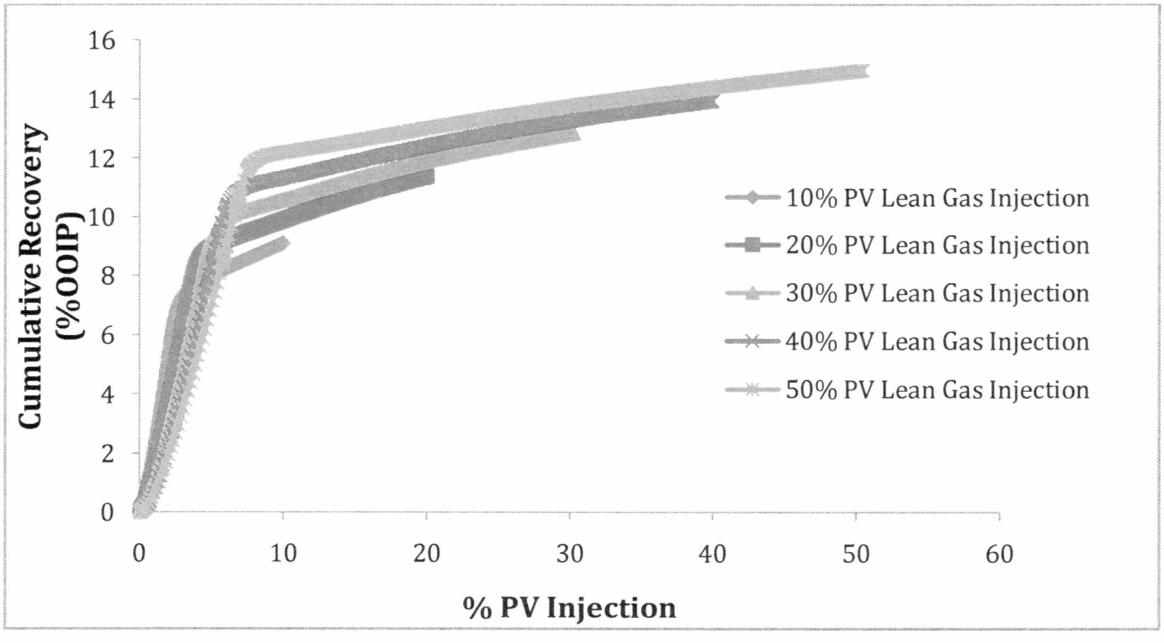

Figure C 2: Recovery plot for lean gas injection

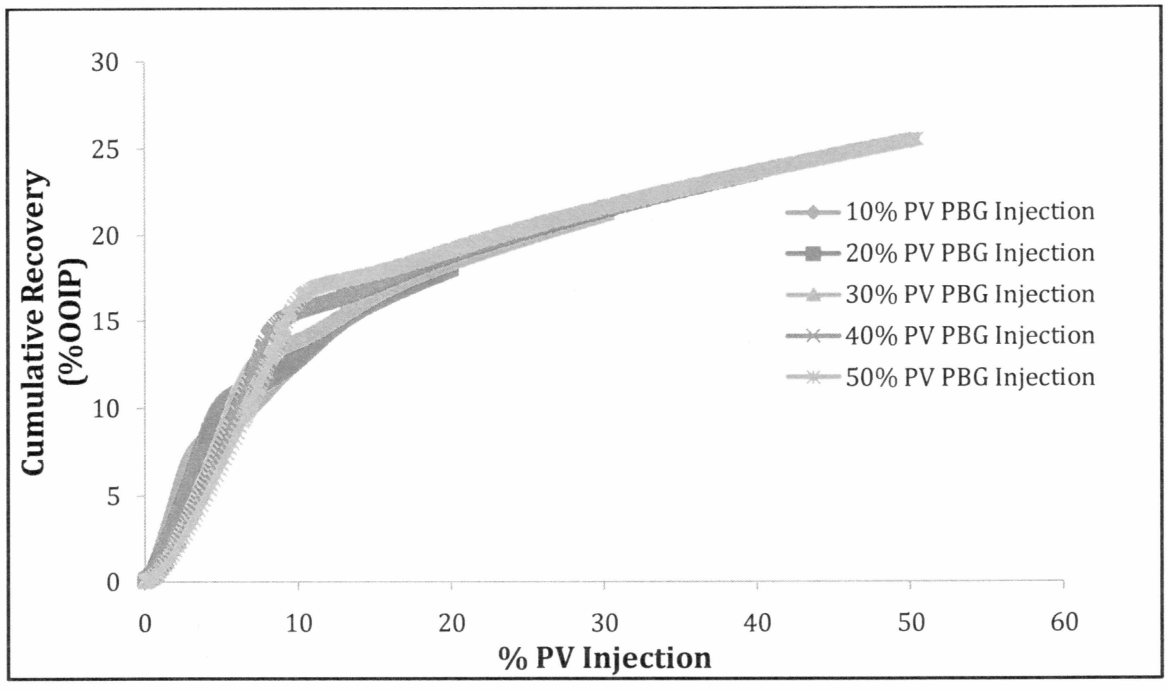

Figure C 3: Recovery plot for PBG injection

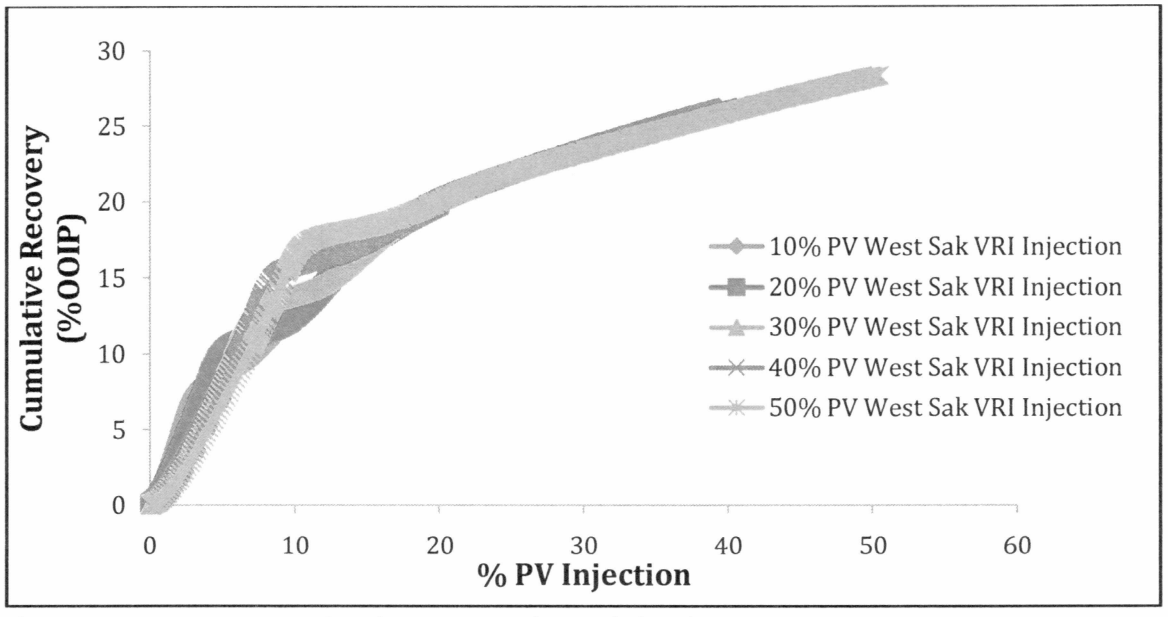

Figure C 4: Recovery plot for West Sak VRI injection